

Supporting Information for: Quadrupolar NMR Crystallography Guided Crystal Structure Prediction (QNMRX-CSP)

Austin A. Peach,^{1,2} Carl H. Fleischer III,^{1,2} Kirill Levin,³ Sean T. Holmes,^{1,2}
Jazmine E. Sanchez,^{1,2} and Robert W. Schurko^{1,2,*}

1. Department of Chemistry and Biochemistry, Florida State University, Tallahassee, FL 32306

2. National High Magnetic Field Laboratory, Tallahassee, FL 32310

3. Department of Chemistry and Biochemistry, McGill University, Montreal, Quebec, Canada, H3A 0G4

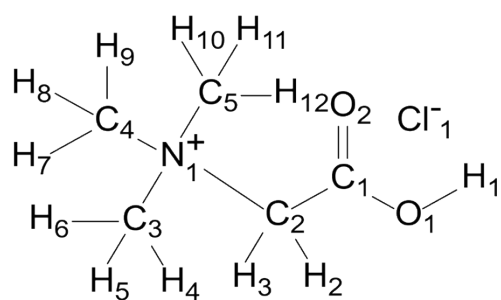
*Author to whom correspondence should be addressed. E-mail: rschurko@fsu.edu; Web: <https://www.chem.fsu.edu/~schurko/>; Tel: 850-645-8614

Table of Contents:

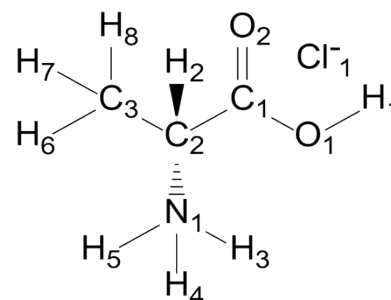
| Figure Column with Title: | Page |
|--|-------|
| Scheme SA. Molecular diagrams with atoms numbered of the five HCl salts involved in benchmarking: betaine HCl, glycine HCl, <i>D</i> -alanine HCl, guanidine HCl, and aminoguanidine HCl. Hirshfeld charges corresponding to each atom are listed in Tables S2 – S6. | 4 |
| Scheme SB. Molecular diagrams with atoms numbered of the two HCl salts involved in blind tests: metformin HCl and <i>N,N'</i> -dimethylglycine HCl. Hirshfeld charges corresponding to each atom are listed in Tables S7 and S8. | 5 |
| Table S1: Charge Database: Hirshfeld charges of atoms in common structural moieties in organic HCl salts for use in the QNMRX-CSP protocol in S2, S3, and S4. | 6 |
| Supplement S1: Workstations | 7 |
| Supplement S2: Charge Database | 8 |
| Table S2. Hirshfeld charges assigned to atoms in a molecular fragment of betaine HCl in the QNMRX-CSP protocol in S1, S2, and S3. | 9 |
| Table S3. Hirshfeld charges assigned to atoms in a molecular fragment of glycine HCl in the QNMRX-CSP protocol in S1, S2, and S3. | 10 |
| Table S4. Hirshfeld charges assigned to atoms in a molecular fragment of <i>D</i> -alanine HCl in the QNMRX-CSP protocol in S1, S2, and S3. | 11 |
| Table S5. Hirshfeld charges assigned to atoms in a molecular fragment of guanidine HCl in the QNMRX-CSP protocol in S1, S2, and S3. | 12 |
| Table S6. Hirshfeld charges assigned to atoms in a molecular fragment of aminoguanidine HCl in the QNMRX-CSP protocol in S1, S2, and S3. | 13 |
| Table S7. Hirshfeld charges assigned to atoms in a molecular fragment of <i>N,N'</i> -dimethylglycine HCl in the QNMRX-CSP protocol in S4. | 14 |
| Table S8. Hirshfeld charges assigned to atoms in a molecular fragment of metformin HCl in the QNMRX-CSP protocol in S4. | 15 |
| Table S9. Comparison of atomic charges for betaine HCl obtained from Hirshfeld and Mulliken population analysis. | 16 |
| Table S10. Validated structural models of betaine HCl from the benchmarking of the QNMRX-CSP protocol in S1, S2, and S3. | 17 |
| Table S11. Validated structural models of glycine HCl from the benchmarking of the QNMRX-CSP protocol in S1, S2, and S3. | 18 |
| Table S12. Validated structural models of <i>D</i> -alanine HCl from the benchmarking of the QNMRX-CSP protocol in S1, S2, and S3. | 19 |
| Table S13. Validated structural models of guanidine HCl from the benchmarking of the QNMRX-CSP protocol in S1, S2, and S3. | 20-21 |
| Table S14. Validated structural models of aminoguanidine HCl from the benchmarking of the QNMRX-CSP protocol in S1, S2, and S3. | 22 |
| Table S15. Structural models of betaine HCl, from the benchmarking of M2 Step 2 from the | 23 |

| | |
|---|----|
| QNMXX-CSP protocol in S1 outside of thresholds for metrics $\Gamma_{\text{EFG}} \leq 0.49$ MHz and $E_{\text{lat}} \leq 50$ kJ mol ⁻¹ . | |
| Supplement S3. Benchmarking structures outside of thresholds in M3 Step 2 of the QNMXX-CSP protocol in S1. | 24 |
| Figure S1. A walkthrough of the QNMXX-CSP protocol, Module 1, Stage 1 (Molecular Fragments and Motion Groups) for glycine HCl. M1 Step 1: obtain a known crystal structure (GLYHCL). M1 Step 2: perform a DFT-D2* geometry optimization and unbuild the crystal structure. M1 Step 3: assign the Hirshfeld charges to the atoms. M1 Step 4: assign the motion groups. | 25 |
| Figure S2. Scatter plots of E_{lat} vs. Γ_{EFG} for the walkthrough of the QNMXX-CSP protocol in Module 3, Stage 1, Steps 1-3 (QNMXX) for glycine HCl: Red and blue points denote discarded and retained candidate structures, respectively. The numbers of structures before (red) and after (blue) the application of benchmarked metrics are shown to the right. Shown in the inset of the scatter plot in M3 Step 3 are the structures that have $E_{\text{lat}} \leq 1$ kJ mol ⁻¹ . | 26 |
| Figure S3. A comparison of the DFT-D2* geometry-optimized structural model of glycine HCl derived from its known crystal structure (GLYHCL) with two (from a set of 4) validated structural models, 10-228 and 10-260. | 27 |
| Figure S4. A walkthrough of the QNMXX-CSP protocol, Module 1, Stage 1 (Molecular Fragments and Motion Groups) for <i>D</i> -alanine HCl. M1 Step 1: obtain a known crystal structure (ALAHCL). M1 Step 2: perform a DFT-D2* geometry optimization and unbuild the crystal structure. M1 Step 3: assign the Hirshfeld charges to the atoms. M1 Step 4: assign the motion groups. | 28 |
| Figure S5. Scatter plots of E_{lat} vs. Γ_{EFG} for the walkthrough of the QNMXX-CSP protocol in Module 3, Stage 1, Steps 1-3 (QNMXX) for <i>D</i> -alanine HCl: Red and blue points denote discarded and retained candidate structures, respectively. The numbers of structures before (red) and after (blue) the application of benchmarked metrics are shown to the right. Shown in the inset of the scatter plot in M3 Step 3 are the structures that have $E_{\text{lat}} \leq 1$ kJ mol ⁻¹ . | 29 |
| Figure S6. A comparison of the DFT-D2* geometry-optimized structural model of <i>D</i> -alanine HCl derived from its known crystal structure (ALAHCL) with two (from a set of 10) validated structural models, 1-329 and 8-489. | 30 |
| Figure S7. A walkthrough of the QNMXX-CSP protocol, Module 1, Stage 1 (Molecular Fragments and Motion Groups) for guanidine HCl. M1 Step 1: obtain a known crystal structure (GUANIDC01). M1 Step 2: perform a DFT-D2* geometry optimization and unbuild the crystal structure. M1 Step 3: assign the Hirshfeld charges to the atoms. M1 Step 4: assign the motion groups. | 31 |
| Figure S8. Scatter plots of E_{lat} vs. Γ_{EFG} for the walkthrough of the QNMXX-CSP protocol in Module 3, Stage 1, Steps 1-3 (QNMXX) for guanidine HCl: Red and blue points denote discarded and retained candidate structures, respectively. The numbers of structures before (red) and after (blue) the application of benchmarked metrics are shown to the right. Shown in the inset of the scatter plot in M3 Step 3 are the structures that have $E_{\text{lat}} \leq 1$ kJ mol ⁻¹ . | 32 |
| Figure S9. A comparison of the DFT-D2* geometry-optimized structural model of guanidine HCl derived from its known crystal structure (GUANIDC01) with two (from a set of 19) validated structural models, 6-198 and 6-226. | 33 |
| Figure S10. A walkthrough of the QNMXX-CSP protocol, Module 1, Stage 1 (Molecular Fragments and Motion Groups) for aminoguanidine HCl. M1 Step 1: obtain a known crystal structure (AMGUAC02). M1 Step 2: perform a DFT-D2* geometry optimization and unbuild the crystal structure. M1 Step 3: assign the Hirshfeld charges to the atoms. M1 Step 4: assign the motion groups. | 34 |
| Figure S11. Scatter plots of E_{lat} vs. Γ_{EFG} for the walkthrough of the QNMXX-CSP protocol in Module 3, Stage 1, Steps 1-3 (QNMXX) for aminoguanidine HCl: Red and blue points denote discarded and retained candidate structures, respectively. The numbers of structures before (red) and after (blue) the application of benchmarked metrics are shown to the right. Shown in the inset of the scatter plot in M3 Step 3 are the structures that have $E_{\text{lat}} \leq 1$ kJ mol ⁻¹ . | 35 |
| Figure S12. A comparison of the DFT-D2* geometry-optimized structural model of aminoguanidine HCl derived from its known crystal structure (AMGUAC02) with two (from a set of 3) validated structural models, 4-27 and 9-107. | 36 |
| Figure S13. A comparison of the DFT-D2* geometry-optimized structural model of betaine HCl derived from its known crystal structure (BETANC01) with one validated structural model each from S2 and S3, 8-114 and 10-269, respectively. | 37 |

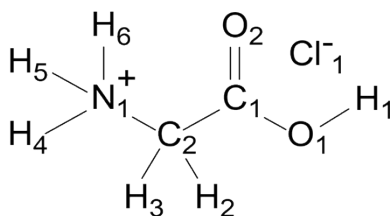
| | |
|--|----|
| Figure S14. A comparison of the DFT-D2* geometry-optimized structural model of glycine HCl derived from its known crystal structure (GLYHCL) with one validated structural model each from S2 and S3, 5-664 and 18-352, respectively. | 38 |
| Figure S15. A comparison of the DFT-D2* geometry-optimized structural model of <i>D</i> -alanine HCl derived from its known crystal structure (ALAHCL) with one validated structural model each from S2 and S3, 7-374 and 14-480, respectively. | 39 |
| Figure S16. A comparison of the DFT-D2* geometry-optimized structural model of guanidine HCl derived from its known crystal structure (GUANIDC01) with one validated structural model each from S2 and S3, 10-266 and 9-221, respectively. | 40 |
| Figure S17. A comparison of the DFT-D2* geometry-optimized structural model of aminoguanidine HCl derived from its known crystal structure (AMGUAC02) with one validated structural model each from S2 and S3, 12-10 and 20-24, respectively. | 41 |
| Figure S18. Molecular fragments of <i>N,N'</i> -dimethylglycine HCl (A, Dmg1 fragment is shown) and two conformers of metformin HCl (B, Met1 and Met2), with Hirshfeld charges and motion groups assigned. | 42 |



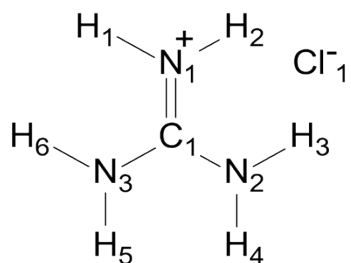
Betaine HCl
(**Bet**)



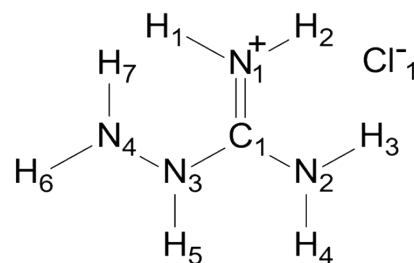
D-Alanine HCl
(**Ala**)



Glycine HCl
(**Gly**)

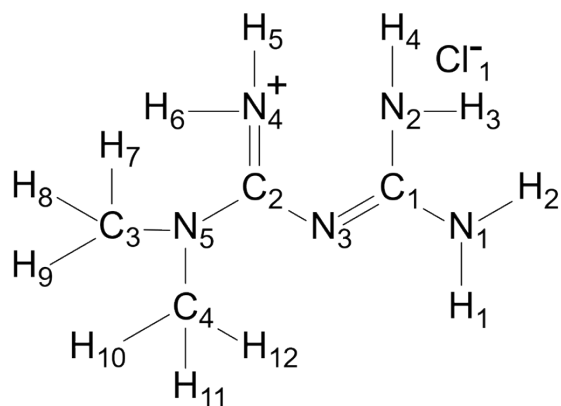


Guanidine HCl
(**Gua**)

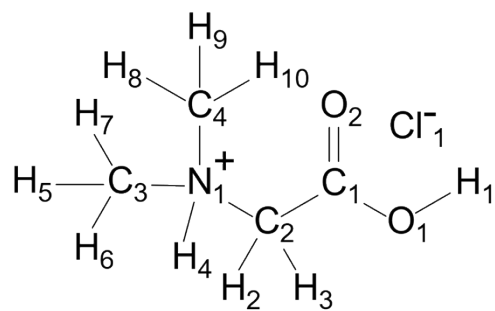


Aminoguanidine HCl
(**Amg**)

Scheme SA. Molecular diagrams with atoms numbered of the five HCl salts involved in benchmarking: betaine HCl, glycine HCl, *D*-alanine HCl, guanidine HCl, and aminoguanidine HCl. Hirshfeld charges corresponding to each atom are listed in **Tables S2 – S6**.



Metformin HCl
(Met)



N,N'-Dimethylglycine HCl
(Dmg)

Scheme SB. Molecular diagrams with atoms numbered of the two HCl salts involved in blind tests: metformin HCl and *N,N'*-dimethylglycine HCl. Hirshfeld charges corresponding to each atom are listed in **Tables S7** and **S8**.

Table S1: Charge Database: Hirshfeld charges of atoms in common structural moieties in organic HCl salts for use in the QNMRX-CSP protocol in S2, S3, and S4.

| Functional Group ^{a,b} | Count | Average ^c | Standard Deviation |
|-----------------------------------|-------|----------------------|--------------------|
| Cl ⁻ | 44 | -0.304 | 0.021 |
| (N)H ₃ ⁺ | 28 | -0.038 | 0.007 |
| N(H) ₃ ⁺ | 84 | 0.104 | 0.008 |
| (C)OOH | 22 | 0.204 | 0.008 |
| C(O)OH | 22 | -0.211 | 0.010 |
| CO(O)H | 22 | -0.132 | 0.004 |
| COO(H) | 22 | 0.103 | 0.008 |
| Alpha C | 24 | 0.022 | 0.013 |
| Alpha H | 25 | 0.044 | 0.006 |
| (N) ⁺ -CH ₃ | 6 | 0.047 | 0.055 |
| N ⁺ -(C)H ₃ | 12 | -0.055 | 0.006 |
| (N)H ₂ | 3 | -0.147 | 0.005 |
| N(H) ₂ | 6 | 0.087 | 0.007 |
| (=N) ^d | 7 | -0.149 | 0.015 |
| (-N)H ₂ ^d | 8 | -0.078 | 0.007 |
| Terminal (-N) ^d | 6 | -0.143 | 0.005 |
| (C) ^d | 7 | 0.189 | 0.012 |
| (H) ^d | 30 | 0.094 | 0.008 |
| N-(C)H ₃ | 3 | -0.063 | 0.005 |
| Other H | 294 | 0.036 | 0.017 |

^a Atoms to which the charge corresponds is in parentheses ().

^b List of HCl salts with CCDC codes used in the development of the charge database: adiphenine HCl (ADIPHC), *L*-alanine HCl (ALAHCL), *L*-arginine HCl monohydrate (ARGHCL10), *DL*-aspartic acid HCl (ASPART10), bicyclomine HCl (BAHDET), betaine HCl (BETANC01), *N,N*-dimethylglycine HCl (BUTNIN), cimetidine HCl monohydrate (CADVIM), *p*-chloroaniline HCl (CURGOL), *L*-cysteine HCl monohydrate (CYSCLM11), *DL*-proline HCl (DLPROL), dopamine HCl (DOPAMN01), cimetidine HCl (EHIWEZ), *L*-leucine HCl monohydrate (FEQYUW), adamantanamine HCl (FINVAZ), guanidinium chloride (GANIDC01), *L*-glutamine HCl (GLUTAN), glycine HCl (GLYHCL), *L*-histidine HCl monohydrate (HISTCM01), diphenhydraminium chloride (JEMJOA), mexiletine HCl (JIZJEH01), *L*-arginine HCl (LARGIN), *L*-glutamic acid HCl (LGLUTA), *L*-glutamic acid HCl (LGLUTA02), *L*-tyrosine HCl (LTYRHC10), *L*-methionine HCl (METHCL), *L*-threoninium chloride (MOVLOZ01), *L*-phenylalanine HCl (PHALNC01), *L*-phenylalanine HCl (PHALNC10), procaine HCl (PROCHC10), procaine HCl (PROCHC11), rantidine HCl (TADZAZ01), *p*-bromoaniline HCl (TAWRAL), *L*-tryptophan HCl (TRYPTC), 2-chloroanilinium chloride (UFAJAM), 3-chloroanilinium chloride (UFAJOA), *L*-valine HCl (VALEHC10), *L*-cysteine methyl ester HCl (VEDCEM), *L*-cysteine ethyl ester HCl (VEDCOW01), *DL*-serine HCl (VOKHEJ), isoprenaline HCl (WELYOB), and tetracaine HCl (XISVOK01).

^c Hirshfeld charges from this database are assigned to atoms in structural models used in S2, S3, and S4 calculations. Alterations to charges were made based on the standard deviation to obtain a net sum of 0 for each structural model.

^d Atoms are from guanidine moieties.

Supplement S1: Workstations

All calculations were run on workstations featuring two Intel® Xeon Silver 4110 processors with a base frequency of 2.10 GHz and 8 cores/16 threads, two NVIDIA Quadro S2000 graphics cards, 192 GB of 2400 MHz RAM, two NVMe solid-state hard drives, one KIOXIA 512 GB (reserved for OS and programs), a Samsung 1024 GB hard drive for data storage, and a Windows 10 Pro operating system.

Using our workstations, the geometry optimization on a gas phase molecule in M1 takes approximately 20 minutes. On average, one trial of M2 requires two hours of computational time to generate the candidate structures. M3 is the most computationally demanding and time-consuming module in the QNMRX-CSP protocol. The first DFT-D2* geometry optimization and calculation of EFG tensors is computationally inexpensive, taking only 15 to 20 minutes per structure; however, the second and third DFT-D2* geometry optimizations and EFG tensor calculations range between 8 – 12 hours per structure. It is worth noting that calculations in M2 and M3 can be run in parallel to reduce computational time.

Supplement S2: Charge Database

In Stage 2, 3, and 4 (S2, S3, S4) calculations, it is necessary to approximate the starting values of the Hirshfeld charges; therefore, we constructed a *Charge Database*. This was accomplished by conducting plane-wave DFT-D2* geometry optimizations to convergence (see §2.1 for details) on structural models of 43 HCl salts with CIF files from the CCDC used as starting points (see **Table S1**). Atoms were grouped together based on their functional groups (*e.g.*, chloride anions, tertiary, secondary, or primary amines, methyl carbons, methyl hydrogens, *etc.*) and the respective average charge was determined. A standard deviation in charge for each atom was calculated, and this was used to modify charges for structural models used in calculations such that the sum of charges for a molecule was zero, while keeping the values of charges as close as possible to those listed in the Charge Database (*e.g.*, chloride anions and hydrogen atoms are adjusted by small amounts, typically ≤ 0.055).

Table S2. Hirshfeld charges assigned to atoms in a molecular fragment of betaine HCl in the QNMRX-CSP protocol in S1, S2, and S3.

| Atom # ^a | S1 Charges | S2/S3 Charges |
|---------------------|------------|---------------|
| H1 | 0.090 | 0.103 |
| H2 | 0.040 | 0.044 |
| H3 | 0.040 | 0.044 |
| H4 | 0.050 | 0.039 |
| H5 | 0.040 | 0.039 |
| H6 | 0.040 | 0.039 |
| H7 | 0.040 | 0.039 |
| H8 | 0.040 | 0.039 |
| H9 | 0.040 | 0.039 |
| H10 | 0.040 | 0.039 |
| H11 | 0.040 | 0.039 |
| H12 | 0.040 | 0.039 |
| C1 | 0.210 | 0.204 |
| C2 | -0.030 | 0.022 |
| C3 | -0.050 | -0.055 |
| C4 | -0.060 | -0.055 |
| C5 | -0.060 | -0.055 |
| N1 | 0.110 | 0.047 |
| O1 | -0.140 | -0.132 |
| O2 | -0.200 | -0.211 |
| C11 | -0.330 | -0.307 |

^a Atom number corresponds to assignments made in **Scheme SA**.

Table S3. Hirshfeld charges assigned to atoms in a molecular fragment of glycine HCl in the QNMRX-CSP protocol in S1, S2, and S3.

| Atom # ^a | S1 Charges | S2/S3 Charges |
|---------------------|------------|---------------|
| H1 | 0.090 | 0.103 |
| H2 | 0.040 | 0.030 |
| H3 | 0.050 | 0.030 |
| H4 | 0.090 | 0.099 |
| H5 | 0.110 | 0.099 |
| H6 | 0.100 | 0.099 |
| C1 | 0.200 | 0.204 |
| C2 | -0.020 | 0.022 |
| N1 | -0.040 | -0.038 |
| O1 | -0.130 | -0.132 |
| O2 | -0.210 | -0.211 |
| C11 | -0.280 | -0.305 |

^a Atom number corresponds to assignments made in **Scheme SA**.

Table S4. Hirshfeld charges assigned to atoms in a molecular fragment of *D*-alanine HCl in the QNMRX-CSP protocol in S1, S2, and S3.

| Atom # ^a | S1 Charges | S2/S3 Charges |
|---------------------|------------|---------------|
| H1 | 0.100 | 0.100 |
| H2 | 0.050 | 0.040 |
| H3 | 0.030 | 0.030 |
| H4 | 0.030 | 0.030 |
| H5 | 0.040 | 0.030 |
| H6 | 0.100 | 0.100 |
| H7 | 0.100 | 0.100 |
| C1 | 0.110 | 0.100 |
| C2 | 0.210 | 0.204 |
| N1 | 0.030 | 0.022 |
| N2 | -0.040 | -0.038 |
| O1 | -0.130 | -0.132 |
| O2 | -0.210 | -0.211 |
| Cl1 | -0.310 | -0.306 |

^a Atom number corresponds to assignments made in **Scheme SA**.

Table S5. Hirshfeld charges assigned to atoms in a molecular fragment of guanidine HCl in the QNMRX-CSP protocol in S1, S2, and S3.

| Atom # ^a | S1 Charges | S2/S3 Charges |
|---------------------|------------|---------------|
| H1 | 0.090 | 0.092 |
| H2 | 0.090 | 0.092 |
| H3 | 0.090 | 0.092 |
| H4 | 0.090 | 0.092 |
| H5 | 0.090 | 0.092 |
| H6 | 0.090 | 0.092 |
| C1 | 0.200 | 0.189 |
| N1 | -0.140 | -0.149 |
| N2 | -0.150 | -0.143 |
| N3 | -0.150 | -0.143 |
| C11 | -0.300 | -0.306 |

^a Atom number corresponds to assignments made in **Scheme SA**.

Table S6. Hirshfeld charges assigned to atoms in a molecular fragment of aminoguanidine HCl in the QNMRX-CSP protocol in S1, S2, and S3.

| Atom # ^a | S1 Charges | S2/S3 Charges |
|---------------------|------------|---------------|
| H1 | 0.090 | 0.087 |
| H2 | 0.090 | 0.087 |
| H3 | 0.080 | 0.087 |
| H4 | 0.070 | 0.087 |
| H5 | 0.070 | 0.087 |
| H6 | 0.100 | 0.087 |
| H7 | 0.100 | 0.087 |
| C1 | 0.190 | 0.189 |
| N1 | -0.150 | -0.149 |
| N2 | -0.150 | -0.150 |
| N3 | -0.050 | -0.050 |
| N4 | -0.140 | -0.143 |
| C11 | -0.300 | -0.306 |

^a Atom number corresponds to assignments made in **Scheme SA**.

Table S7. Hirshfeld charges assigned to atoms in a molecular fragment of *N,N'*-dimethylglycine HCl in the QNMRX-CSP protocol in S4.

| Atom # ^a | Charge |
|---------------------|--------|
| H1 | 0.103 |
| H2 | 0.044 |
| H3 | 0.044 |
| H4 | 0.104 |
| H5 | 0.031 |
| H6 | 0.031 |
| H7 | 0.031 |
| H8 | 0.031 |
| H9 | 0.031 |
| H10 | 0.031 |
| C1 | 0.204 |
| C2 | 0.022 |
| C3 | -0.055 |
| C4 | -0.055 |
| N1 | 0.047 |
| O1 | -0.132 |
| O2 | -0.211 |
| Cl1 | -0.301 |

^a Atom number corresponds to assignments made in **Scheme SB**.

Table S8. Hirshfeld charges assigned to atoms in a molecular fragment of metformin HCl in the QNMRX-CSP protocol in S4.

| Atom # ^a | Charge |
|---------------------|--------|
| H1 | 0.090 |
| H2 | 0.090 |
| H3 | 0.090 |
| H4 | 0.090 |
| H5 | 0.090 |
| H6 | 0.090 |
| H7 | 0.030 |
| H8 | 0.030 |
| H9 | 0.030 |
| H10 | 0.030 |
| H11 | 0.030 |
| H12 | 0.030 |
| C1 | 0.189 |
| C2 | 0.189 |
| C3 | -0.063 |
| C4 | -0.063 |
| N1 | -0.143 |
| N2 | -0.143 |
| N3 | -0.149 |
| N4 | -0.149 |
| N5 | -0.078 |
| Cl1 | -0.310 |

^a Atom number corresponds to assignments made in **Scheme SB**.

Table S9. Comparison of atomic charges for betaine HCl obtained from Hirshfeld and Mulliken population analysis.

| Atom # ^a | Hirshfeld | Mulliken |
|---------------------|-----------|----------|
| H1 | 0.090 | 0.490 |
| H2 | 0.040 | 0.360 |
| H3 | 0.040 | 0.330 |
| H4 | 0.050 | 0.310 |
| H5 | 0.040 | 0.340 |
| H6 | 0.040 | 0.320 |
| H7 | 0.040 | 0.310 |
| H8 | 0.040 | 0.310 |
| H9 | 0.040 | 0.330 |
| H10 | 0.040 | 0.310 |
| H11 | 0.040 | 0.310 |
| H12 | 0.040 | 0.320 |
| C1 | 0.210 | 0.700 |
| C2 | -0.030 | -0.480 |
| C3 | -0.050 | -0.700 |
| C4 | -0.060 | -0.700 |
| C5 | -0.060 | -0.680 |
| N1 | 0.110 | -0.140 |
| O1 | -0.140 | -0.670 |
| O2 | -0.20 | -0.600 |
| Cl1 | -0.330 | -0.750 |

^a Atom number corresponds to assignments made in **Scheme SA**.

Table S10. Validated structural models of betaine HCl from the benchmarking of the QNMRX-CSP protocol in S1, S2, and S3.

| Stage | Structural Model ^a | Γ_{EFG} (MHz) ^b | E_{lat} (kJ mol ⁻¹) ^c | R (%) ^d | RMSD (Å) ^e |
|-------|-------------------------------|--|---|----------------------|-----------------------|
| 1 | 2-320 | 0.325 | 0.000 | 1.387 | 0.112 |
| 1 | 2-486 | 0.323 | 0.010 | 1.461 | 0.113 |
| 1 | 9-632 | 0.321 | 0.010 | 1.135 | 0.003 |
| 1 | 9-158 | 0.323 | 0.019 | 1.936 | 0.111 |
| 1 | 2-330 | 0.331 | 0.029 | 2.253 | 0.110 |
| 1 | 2-494 | 0.320 | 0.039 | 1.549 | 0.112 |
| 1 | 4-272 | 0.328 | 0.039 | 2.017 | 0.002 |
| 1 | 2-313 | 0.328 | 0.048 | 2.035 | 0.119 |
| 1 | 4-46 | 0.326 | 0.048 | 2.059 | 0.003 |
| 1 | 7-75 | 0.332 | 0.048 | 2.534 | 0.002 |
| 1 | 10-105 | 0.329 | 0.048 | 2.024 | 0.114 |
| 1 | 8-152 | 0.319 | 0.048 | 1.765 | 0.114 |
| 1 | 10-47 | 0.327 | 0.058 | 1.843 | 0.113 |
| 1 | 5-98 | 0.321 | 0.077 | 1.952 | 0.004 |
| 1 | 2-326 | 0.332 | 0.096 | 1.955 | 0.113 |
| 1 | 10-103 | 0.317 | 0.106 | 1.737 | 0.113 |
| 2 | 8-84 | 0.325 | 0.000 | 1.490 | 0.003 |
| 2 | 2-419 | 0.327 | 0.000 | 1.700 | 0.112 |
| 2 | 10-126 | 0.327 | 0.000 | 1.445 | 0.113 |
| 2 | 4-265 | 0.328 | 0.000 | 1.853 | 0.110 |
| 2 | 2-165 | 0.327 | 0.010 | 1.731 | 0.002 |
| 2 | 4-253 | 0.330 | 0.010 | 1.774 | 0.002 |
| 2 | 4-417 | 0.332 | 0.029 | 1.902 | 0.111 |
| 2 | 8-522 | 0.330 | 0.029 | 1.752 | 0.110 |
| 2 | 8-114 | 0.315 | 0.096 | 1.175 | 0.005 |
| 2 | 4-406 | 0.336 | 0.154 | 1.610 | 0.005 |
| 3 | 8-122 | 0.329 | 0.000 | 1.781 | 0.112 |
| 3 | 8-1660 | 0.324 | 0.000 | 1.565 | 0.112 |
| 3 | 4-1672 | 0.332 | 0.010 | 1.801 | 0.112 |
| 3 | 10-262 | 0.322 | 0.019 | 1.529 | 0.003 |
| 3 | 10-165 | 0.335 | 0.029 | 1.521 | 0.113 |
| 3 | 6-220 | 0.320 | 0.029 | 1.497 | 0.113 |
| 3 | 9-274 | 0.321 | 0.039 | 1.669 | 0.113 |
| 3 | 10-269 | 0.319 | 0.048 | 1.834 | 0.111 |
| 3 | 7-371 | 0.330 | 0.059 | 2.029 | 0.004 |
| 3 | 7-248 | 0.332 | 0.059 | 1.761 | 0.113 |
| 3 | 7-234 | 0.327 | 0.068 | 1.732 | 0.113 |
| 3 | 1-174 | 0.326 | 0.087 | 1.605 | 0.004 |

^a The structural model notation is defined as the *trial number-structure number*. ^b Γ_{EFG} is the EFG distance; see §2.5 and Eqs. (2) and (3) for further information. ^c E_{lat} is the static lattice energy of the structural model, normalized to that of the lowest energy structure, which is assigned a value of $E_{\text{lat}} = 0$ kJ mol⁻¹. ^d R is the R -factor, $R = \Sigma|F_o - F_c| / \Sigma|F_o| \times 100\%$. ^e RMSD is the root-mean squared distance, which is a measure of the distance between corresponding atomic positions and bond angles from the reported crystal structure and candidate structural model(s).

Table S11. Validated structural models of glycine HCl from the benchmarking of the QNMRX-CSP protocol in S1, S2, and S3.

| Stage | Structural Model ^a | Γ_{EFG} (MHz) ^b | E_{lat} (kJ mol ⁻¹) ^c | R (%) ^d | RMSD (Å) ^e |
|-------|-------------------------------|--|---|----------------------|-----------------------|
| 1 | 10-260 | 0.441 | 0.000 | 1.254 | 0.024 |
| 1 | 10-228 | 0.483 | 0.029 | 2.455 | 0.015 |
| 2 | 5-664 | 0.429 | 0.013 | 1.447 | 0.019 |
| 2 | 10-207 | 0.431 | 0.015 | 1.381 | 0.020 |
| 2 | 10-199 | 0.433 | 0.015 | 1.491 | 0.020 |
| 2 | 10-169 | 0.447 | 0.000 | 1.523 | 0.013 |
| 2 | 5-460 | 0.457 | 0.012 | 1.383 | 0.020 |
| 2 | 9-469 | 0.464 | 0.006 | 1.645 | 0.021 |
| 3 | 18-352 | 0.455 | 0.000 | 2.173 | 0.021 |

^{a,b,c,d,e} See footnotes of **Table S10**.

Table S12. Validated structural models of *D*-alanine HCl from the benchmarking of the QNMRX-CSP protocol in S1, S2, and S3.

| Stage | Structural Model ^a | Γ_{EFG} (MHz) ^b | E_{lat} (kJ mol ⁻¹) ^c | R (%) ^d | RMSD (Å) ^e |
|-------|-------------------------------|--|---|----------------------|-----------------------|
| 1 | 8-489 | 0.197 | 0.000 | 0.561 | 0.005 |
| 1 | 5-454 | 0.198 | 0.005 | 0.876 | 0.007 |
| 1 | 9-254 | 0.193 | 0.014 | 0.980 | 0.008 |
| 1 | 5-549 | 0.212 | 0.017 | 0.685 | 0.009 |
| 1 | 1-329 | 0.215 | 0.021 | 0.895 | 0.010 |
| 1 | 9-308 | 0.189 | 0.023 | 2.450 | 0.018 |
| 1 | 8-382 | 0.211 | 0.023 | 1.437 | 0.011 |
| 1 | 10-265 | 0.192 | 0.028 | 0.300 | 0.002 |
| 1 | 7-541 | 0.200 | 0.044 | 2.021 | 0.015 |
| 1 | 8-427 | 0.193 | 0.049 | 1.549 | 0.010 |
| 2 | 7-374 | 0.190 | 0.000 | 1.336 | 0.010 |
| 2 | 3-452 | 0.197 | 0.018 | 2.388 | 0.018 |
| 2 | 1-179 | 0.220 | 0.027 | 1.343 | 0.011 |
| 3 | 18-571 | 0.318 | 0.000 | 9.125 | 0.061 |
| 3 | 18-262 | 0.319 | 0.000 | 9.186 | 0.061 |
| 3 | 14-480 | 0.128 | 0.262 | 8.983 | 0.068 |
| 3 | 14-492 | 0.131 | 0.265 | 9.087 | 0.068 |

^{a,b,c,d,e} See footnotes of **Table S10**.

Table S13. Validated structural models of guanidine HCl from the benchmarking of the QNMRX-CSP protocol in S1, S2, and S3.

| Stage | Structural Model ^a | Γ_{EFG} (MHz) ^b | E_{lat} (kJ mol ⁻¹) ^c | R (%) ^d | RMSD (Å) ^e |
|-------|-------------------------------|--|---|----------------------|-----------------------|
| 1 | 6-271 | 0.348 | 0.000 | 2.941 | 0.056 |
| 1 | 5-354 | 0.385 | 0.154 | 2.600 | 0.035 |
| 1 | 8-209 | 0.390 | 0.164 | 1.630 | 0.035 |
| 1 | 6-188 | 0.363 | 0.202 | 3.793 | 0.030 |
| 1 | 5-311 | 0.391 | 0.212 | 1.548 | 0.033 |
| 1 | 5-434 | 0.406 | 0.270 | 2.219 | 0.035 |
| 1 | 4-38 | 0.413 | 0.289 | 2.827 | 0.038 |
| 1 | 6-226 | 0.383 | 0.366 | 1.326 | 0.022 |
| 1 | 8-242 | 0.443 | 0.434 | 5.006 | 0.044 |
| 1 | 7-228 | 0.446 | 0.463 | 4.870 | 0.042 |
| 1 | 6-198 | 0.366 | 0.472 | 3.062 | 0.019 |
| 1 | 9-407 | 0.450 | 0.482 | 6.106 | 0.052 |
| 1 | 8-174 | 0.455 | 0.501 | 6.303 | 0.050 |
| 1 | 8-260 | 0.446 | 0.511 | 6.269 | 0.053 |
| 1 | 4-209 | 0.471 | 0.530 | 6.751 | 0.050 |
| 1 | 5-291 | 0.453 | 0.559 | 6.898 | 0.054 |
| 1 | 6-182 | 0.476 | 0.646 | 7.300 | 0.049 |
| 1 | 5-191 | 0.479 | 0.771 | 7.468 | 0.044 |
| 1 | 8-132 | 0.473 | 0.849 | 6.130 | 0.043 |
| 2 | 10-232 | 0.425 | 0.000 | 0.809 | 0.050 |
| 2 | 5-44 | 0.424 | 0.000 | 0.372 | 0.006 |
| 2 | 6-261 | 0.420 | 0.000 | 0.556 | 0.003 |
| 2 | 7-206 | 0.418 | 0.000 | 0.519 | 0.003 |
| 2 | 10-182 | 0.422 | 0.009 | 0.670 | 0.006 |
| 2 | 4-385 | 0.430 | 0.009 | 1.196 | 0.009 |
| 2 | 5-340 | 0.422 | 0.009 | 1.215 | 0.008 |
| 2 | 5-360 | 0.427 | 0.009 | 0.751 | 0.007 |
| 2 | 9-282 | 0.423 | 0.009 | 0.352 | 0.003 |
| 2 | 2-254 | 0.435 | 0.019 | 0.801 | 0.004 |
| 2 | 3-230 | 0.429 | 0.019 | 1.284 | 0.007 |
| 2 | 5-322 | 0.425 | 0.019 | 1.250 | 0.008 |
| 2 | 6-279 | 0.420 | 0.019 | 0.854 | 0.005 |
| 2 | 9-318 | 0.432 | 0.019 | 1.439 | 0.006 |
| 2 | 5-70 | 0.428 | 0.028 | 1.223 | 0.009 |
| 2 | 6-243 | 0.416 | 0.028 | 1.386 | 0.008 |
| 2 | 6-271 | 0.424 | 0.028 | 1.958 | 0.010 |
| 2 | 6-32 | 0.421 | 0.028 | 1.558 | 0.009 |
| 2 | 3-36 | 0.428 | 0.038 | 2.254 | 0.110 |
| 2 | 4-258 | 0.419 | 0.038 | 1.916 | 0.009 |
| 2 | 7-181 | 0.422 | 0.038 | 2.311 | 0.010 |
| 2 | 5-241 | 0.438 | 0.048 | 2.740 | 0.011 |
| 2 | 5-287 | 0.426 | 0.048 | 1.902 | 0.010 |
| 2 | 5-295 | 0.427 | 0.048 | 2.624 | 0.011 |
| 2 | 5-37 | 0.422 | 0.048 | 2.223 | 0.011 |
| 2 | 5-378 | 0.428 | 0.048 | 1.169 | 0.009 |
| 2 | 7-119 | 0.431 | 0.048 | 2.584 | 0.012 |
| 2 | 9-291 | 0.429 | 0.048 | 1.003 | 0.008 |
| 2 | 6-27 | 0.424 | 0.057 | 2.461 | 0.012 |
| 2 | 5-327 | 0.417 | 0.057 | 1.988 | 0.013 |
| 2 | 6-217 | 0.427 | 0.057 | 2.667 | 0.012 |

| | | | | | |
|---|--------|-------|-------|-------|-------|
| 2 | 10-266 | 0.406 | 0.067 | 0.985 | 0.008 |
| 2 | 3-268 | 0.419 | 0.067 | 2.243 | 0.011 |
| 2 | 1-427 | 0.436 | 0.077 | 1.121 | 0.003 |
| 2 | 6-199 | 0.427 | 0.077 | 3.239 | 0.013 |
| 2 | 4-286 | 0.427 | 0.096 | 1.968 | 0.014 |
| 2 | 4-365 | 0.439 | 0.096 | 3.284 | 0.015 |
| 2 | 7-137 | 0.432 | 0.096 | 2.809 | 0.013 |
| 2 | 3-344 | 0.427 | 0.106 | 3.163 | 0.016 |
| 2 | 4-38 | 0.438 | 0.106 | 3.583 | 0.016 |
| 2 | 7-164 | 0.433 | 0.106 | 3.211 | 0.015 |
| 2 | 7-165 | 0.438 | 0.115 | 3.742 | 0.017 |
| 2 | 9-294 | 0.437 | 0.125 | 3.073 | 0.016 |
| 2 | 6-160 | 0.438 | 0.135 | 3.812 | 0.017 |
| 2 | 6-197 | 0.433 | 0.144 | 3.893 | 0.018 |
| 2 | 5-258 | 0.440 | 0.154 | 4.353 | 0.019 |
| 2 | 7-214 | 0.426 | 0.212 | 3.924 | 0.021 |
| 3 | 4-252 | 0.433 | 0.000 | 1.520 | 0.008 |
| 3 | 3-136 | 0.430 | 0.028 | 2.169 | 0.009 |
| 3 | 1-230 | 0.419 | 0.038 | 0.905 | 0.009 |
| 3 | 9-221 | 0.417 | 0.028 | 1.150 | 0.005 |
| 3 | 6-110 | 0.422 | 0.038 | 2.429 | 0.009 |
| 3 | 4-322 | 0.424 | 0.048 | 1.982 | 0.011 |

a,b,c,d,e See footnotes of **Table S10**.

Table S14. Validated structural models of aminoguanidine HCl from the benchmarking of the QNMRX-CSP protocol in S1, S2, and S3.

| Stage | Structural Model ^a | Γ_{EFG} (MHz) ^b | E_{lat} (kJ mol ⁻¹) ^c | R (%) ^d | RMSD (Å) ^e |
|-------|-------------------------------|--|---|----------------------|-----------------------|
| 1 | 9-107 | 0.306 | 0.000 | 1.024 | 0.006 |
| 1 | 4-27 | 0.299 | 0.000 | 1.346 | 0.003 |
| 1 | 4-140 | 0.309 | 0.008 | 1.098 | 0.008 |
| 2 | 12-10 | 0.301 | 0.000 | 1.060 | 0.006 |
| 3 | 20-24 | 0.317 | 0.000 | 1.271 | 0.009 |

^{a,b,c,d,e} See footnotes of **Table S10**.

Table S15. Structural models of betaine HCl, from the benchmarking of M3 Step 2 from the QNMRX-CSP protocol in S1 outside of thresholds for metrics $\Gamma_{\text{EFG}} \leq 0.49$ MHz or $E_{\text{lat}} \leq 50$ kJ mol⁻¹.

| Structural Model ^a | Γ_{EFG} (MHz) ^b | E_{lat} (kJ mol ⁻¹) ^c | R (%) ^d | RMSD (Å) ^e |
|-------------------------------|--|---|----------------------|-----------------------|
| 2-320 ^f | 0.118 | 9.181 | 0.833 | 0.431 |
| 7-1033 | 0.532 | 47.527 | 130.070 | 0.747 |
| 9-613 | 1.006 | 7.383 | 153.270 | 0.290 |
| 2-864 | 1.174 | 20.600 | 191.040 | 0.470 |
| 8-1431 | 0.184 | 86.766 | 226.874 | 0.394 |
| 10-456 | 0.482 | 77.146 | 175.023 | 0.650 |

^{a,b,c,d,e} See footnotes of **Table S10**. ^f Lowest energy structural model from M3 Step 3.

Supplement S3. An examination of structural models with metrics outside of thresholds in M3 Step 2 of the QNMRX-CSP protocol in S1.

Structural models outside of thresholds for metrics $\Gamma_{\text{EFG}} \leq 0.49$ MHz and $E_{\text{lat}} \leq 50$ kJ mol⁻¹ (**Table S15**) in M3 Step 2 were selected for testing to see if those that fall outside of the benchmarked metrics still yield valid structural models. These structural models were subjected to M3 Step 3, in which (i) their unit cell parameters were adjusted to match that of the known crystal structure; and (ii) a DFT-D2* geometry optimization to convergence was conducted. In rare cases, these structural models converge and are in agreement with experimental structures. However, in weighing the retention of these rare structural models against those that pass benchmarking metrics, it is apparent that too much additional computational time must be allocated for the former; hence, the benchmarking metrics stand as an optimal method for selecting the best structural models.

Figures

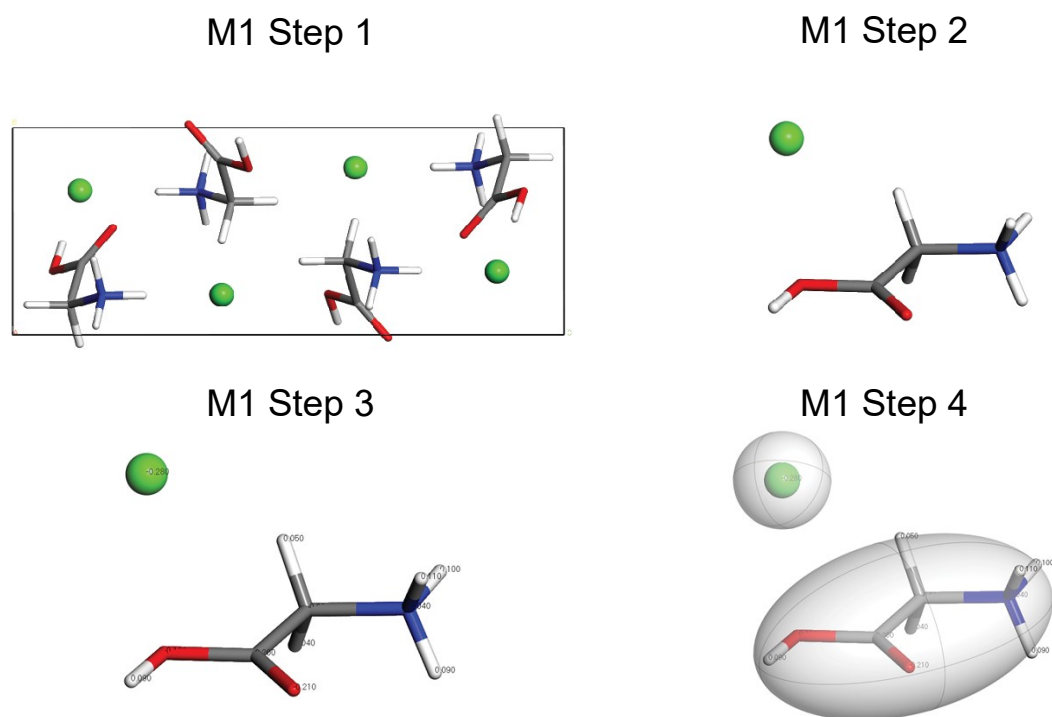


Figure S1. A walkthrough of the QNMXR-CSP protocol, Module 1, Stage 1 (Molecular Fragments and Motion Groups) for glycine HCl. M1 Step 1: obtain a known crystal structure (GLYHCL). M1 Step 2: perform a DFT-D2* geometry optimization and unbuild the crystal structure. M1 Step 3: assign the Hirshfeld charges to the atoms. M1 Step 4: assign the motion groups.

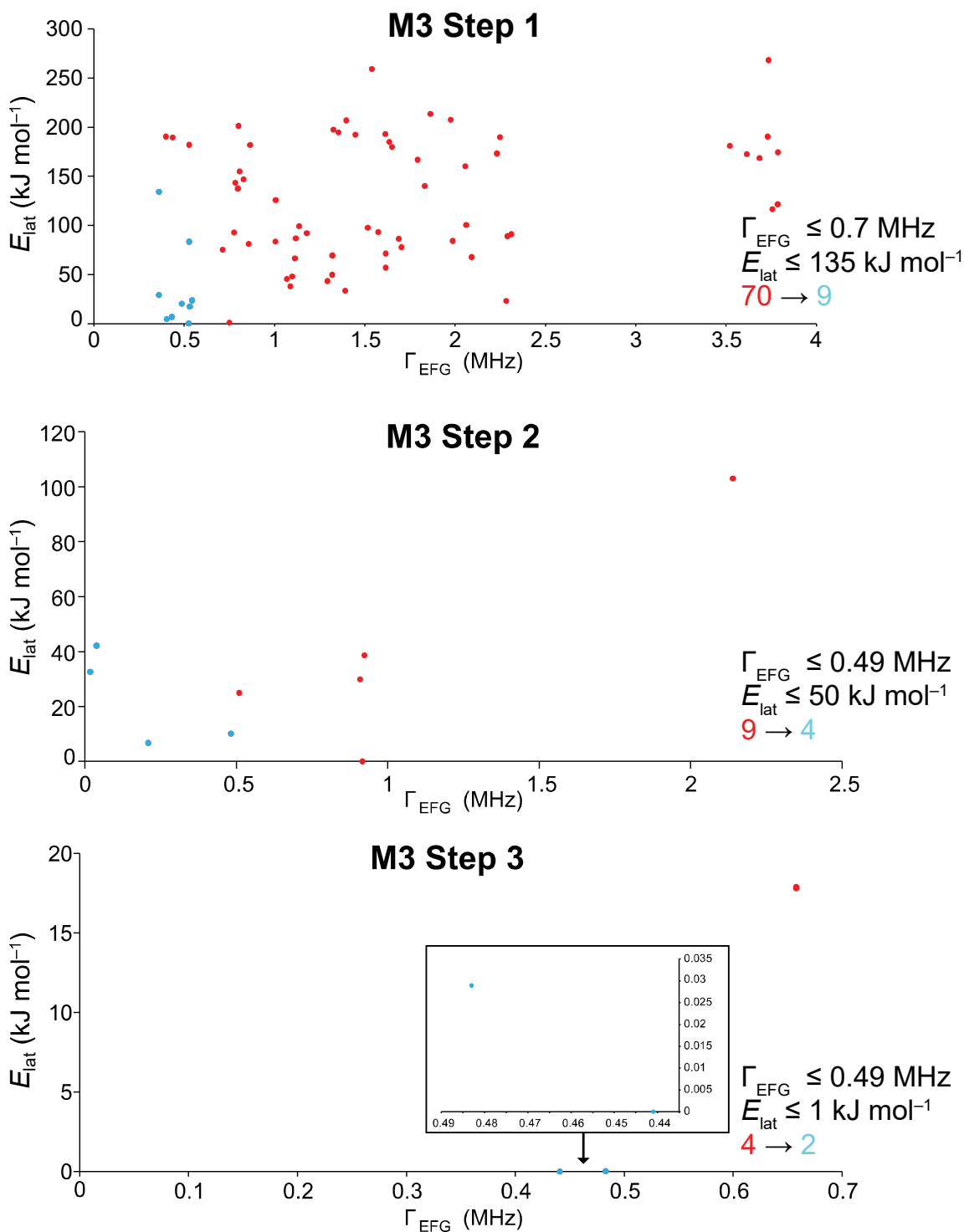


Figure S2. Scatter plots of E_{lat} vs. Γ_{EFG} for the walkthrough of the QNMXR-CSP protocol in Module 3, Stage 1, Steps 1-3 (QNMXR) for glycine HCl: Red and blue points denote discarded and retained candidate structures, respectively. The numbers of structures before (red) and after (blue) the application of benchmarked metrics are shown to the right. Shown in the inset of the scatter plot in M3 Step 3 are the structures that have $E_{\text{lat}} \leq 1$ kJ mol⁻¹.

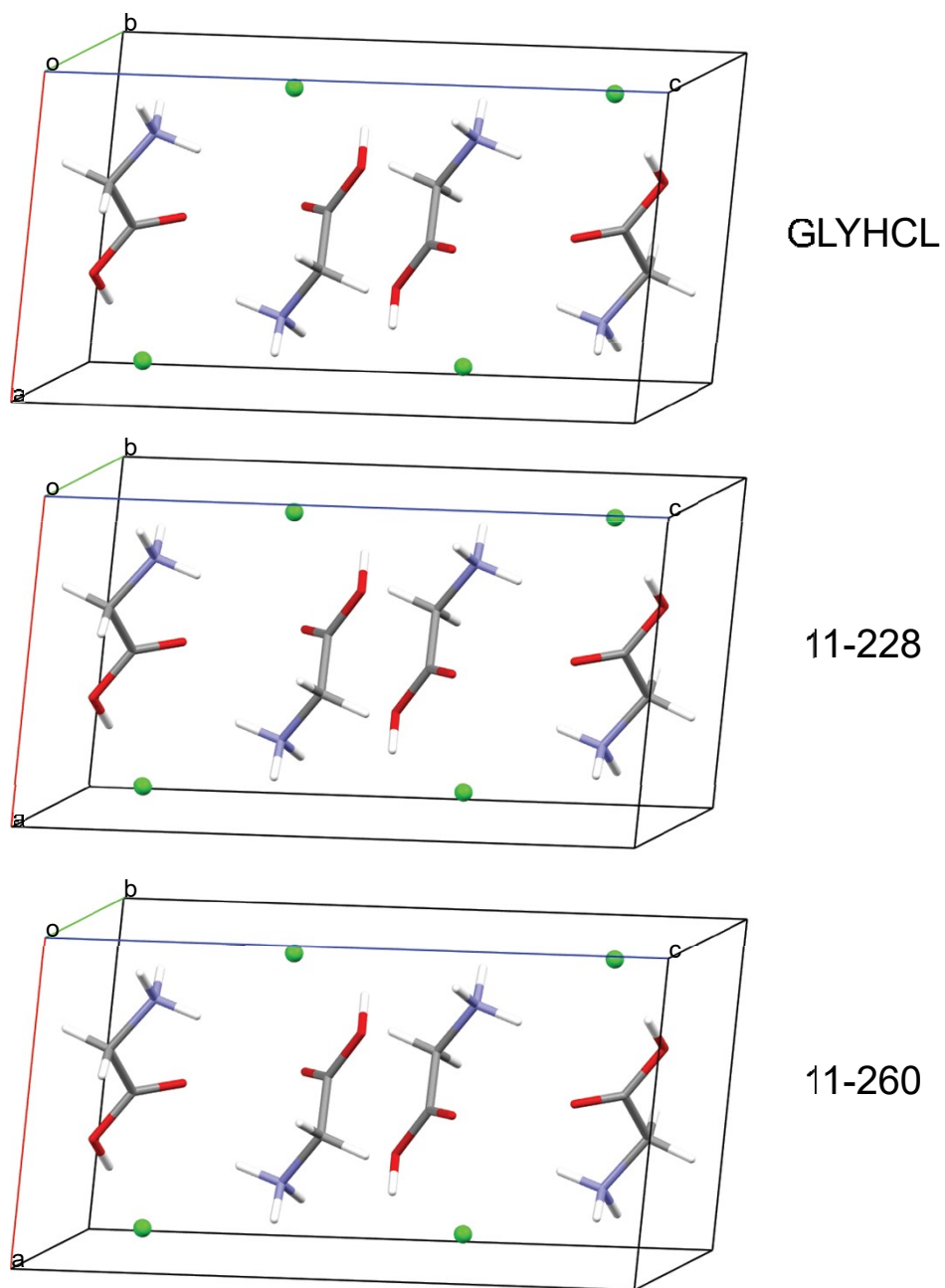


Figure S3. A comparison of the DFT-D2* geometry-optimized structural model of glycine HCl derived from its known crystal structure (GLYHCL) with two (from a set of 4) validated structural models, 10-228 and 10-260.

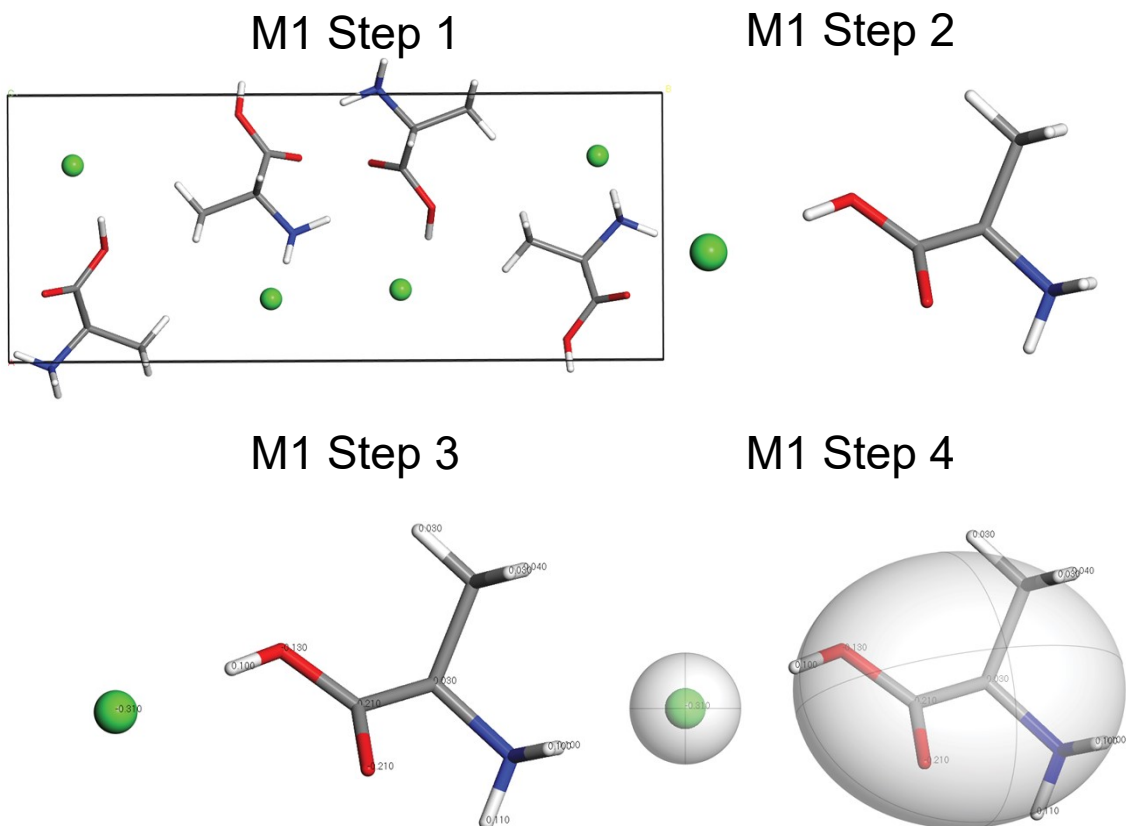


Figure S4. A walkthrough of the QNMXR-CSP protocol, Module 1, Stage 1 (Molecular Fragments and Motion Groups) for *D*-alanine HCl. M1 Step 1: obtain a known crystal structure (ALAHCL). M1 Step 2: perform a DFT-D2* geometry optimization and unbuild the crystal structure. M1 Step 3: assign the Hirshfeld charges to the atoms. M1 Step 4: assign the motion groups.

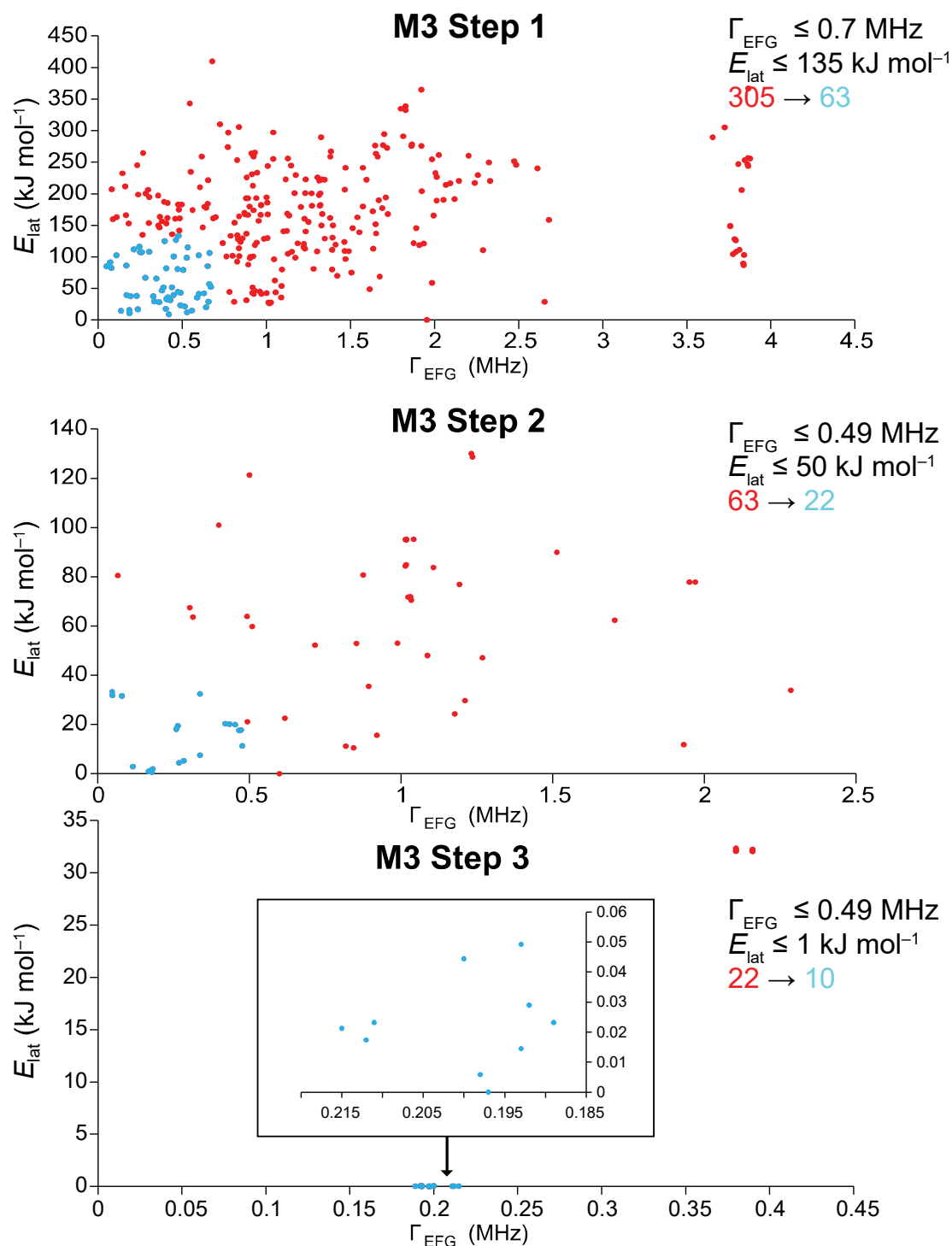


Figure S5. Scatter plots of E_{lat} vs. Γ_{EFG} for the walkthrough of the QNMXR-CSP protocol in Module 3, Stage 1, Steps 1-3 (QNMXR) for *D*-alanine HCl: Red and blue points denote discarded and retained candidate structures, respectively. The numbers of structures before (red) and after (blue) the application of benchmarked metrics are shown to the right. Shown in the inset of the scatter plot in M3 Step 3 are the structures that have $E_{\text{lat}} \leq 1 \text{ kJ mol}^{-1}$.

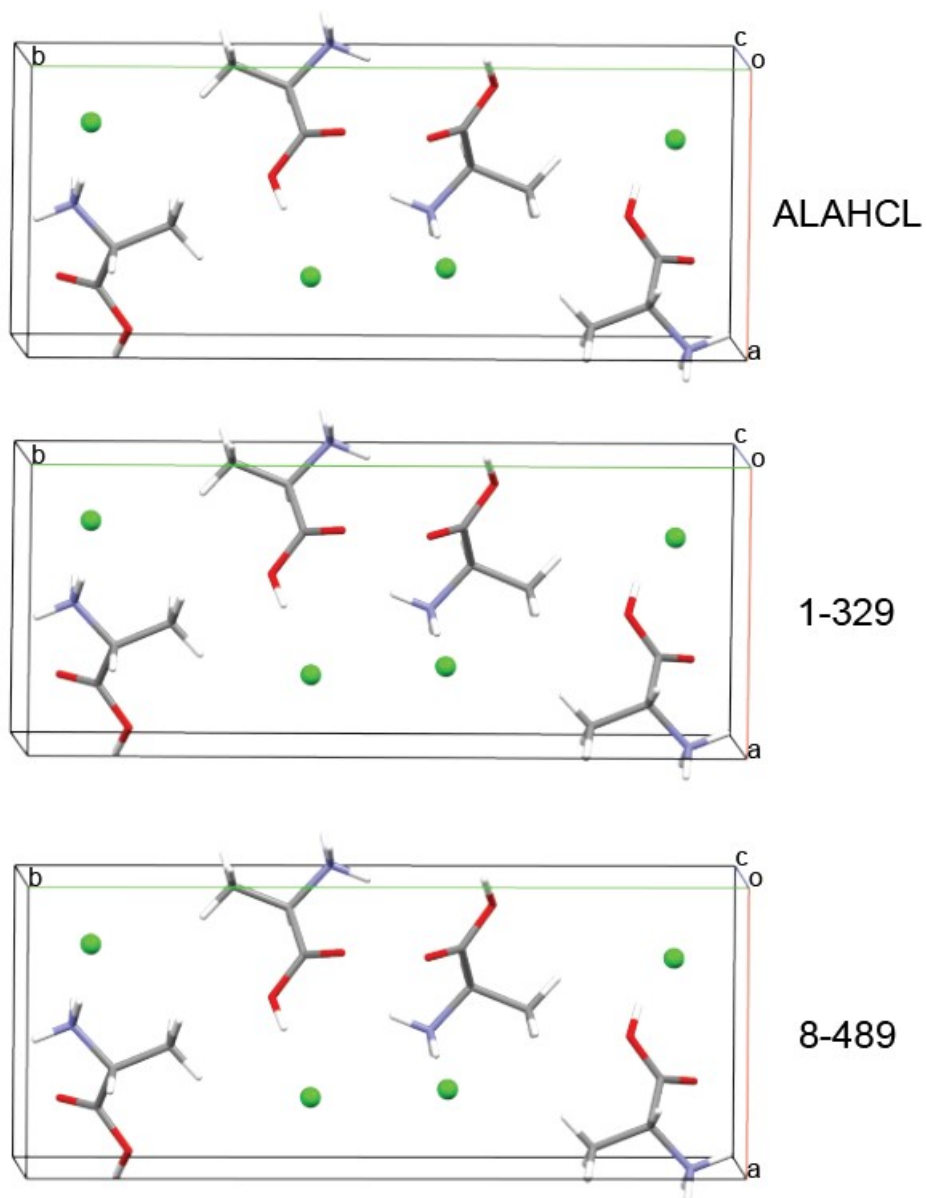


Figure S6. A comparison of the DFT-D2* geometry-optimized structural model of *D*-alanine HCl derived from its known crystal structure (ALAHCL) with two (from a set of 10) validated structural models, 1-329 and 8-489.

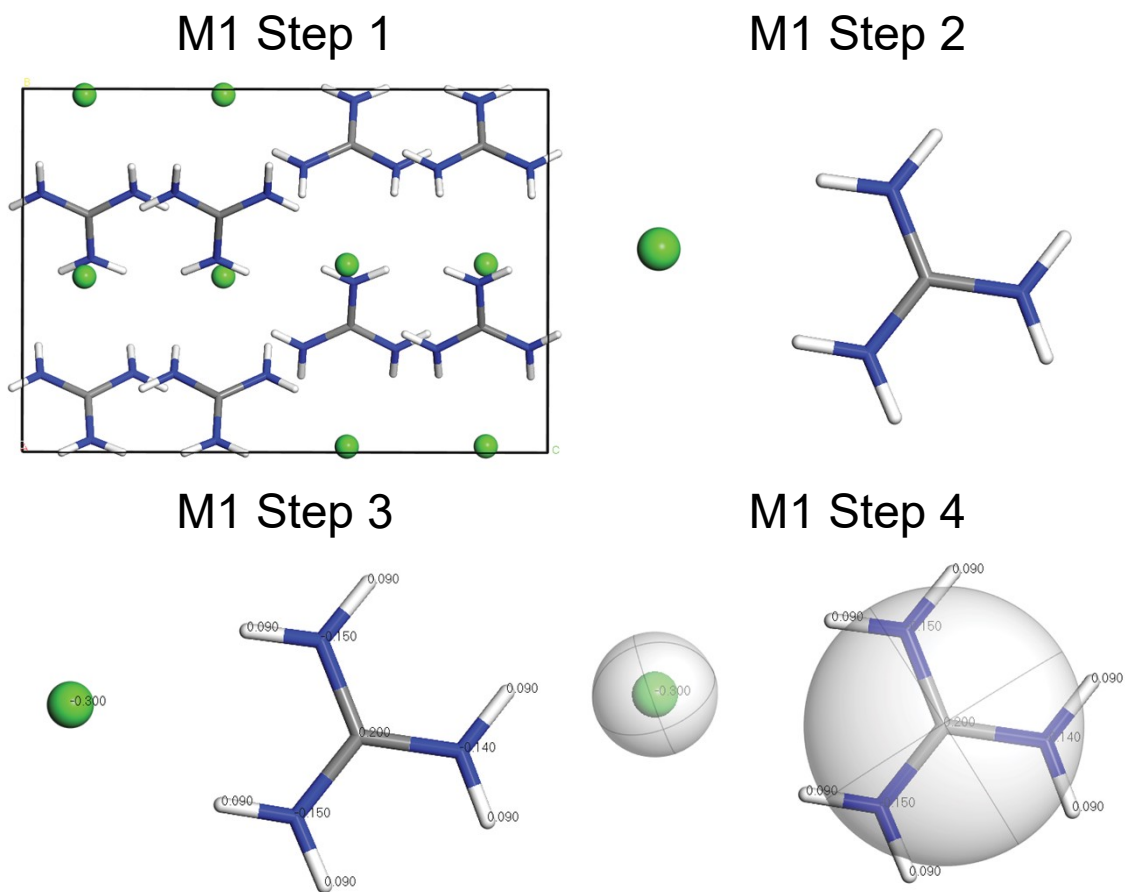


Figure S7. A walkthrough of the QNMXR-CSP protocol, Module 1, Stage 1 (Molecular Fragments and Motion Groups) for guanidine HCl. M1 Step 1: obtain a known crystal structure (GUANIDC01). M1 Step 2: perform a DFT-D2* geometry optimization and unbuild the crystal structure. M1 Step 3: assign the Hirshfeld charges to the atoms. M1 Step 4: assign the motion groups.

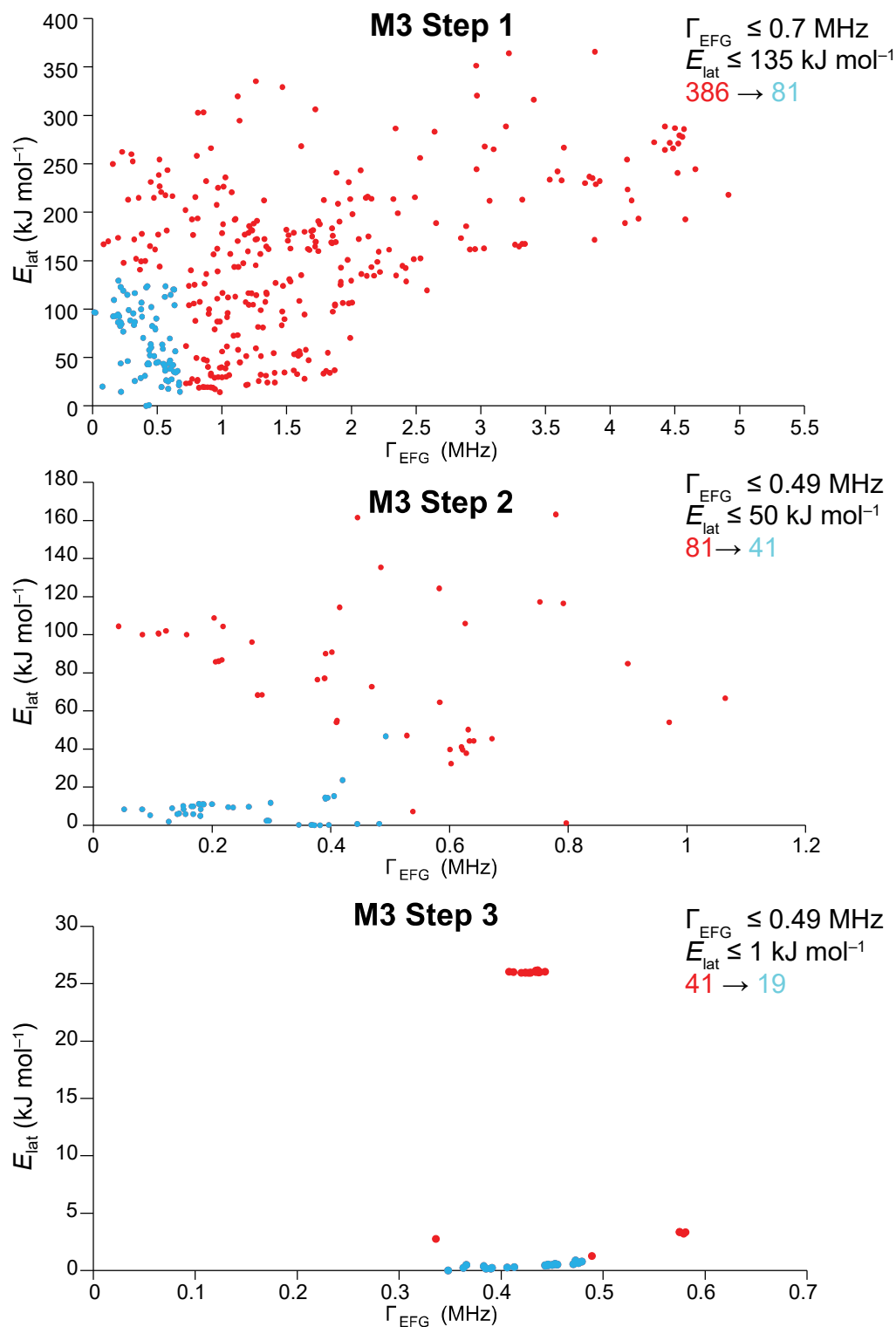


Figure S8. Scatter plots of E_{lat} vs. Γ_{EFG} for the walkthrough of the QNMXR-CSP protocol in Module 3, Stage 1, Steps 1-3 (QNMRX) for guanidine HCl: Red and blue points denote discarded and retained candidate structures, respectively. The numbers of structures before (red) and after (blue) the application of benchmarked metrics are shown to the right. Shown in the inset of the scatter plot in M3 Step 3 are the structures that have $E_{\text{lat}} \leq 1 \text{ kJ mol}^{-1}$.

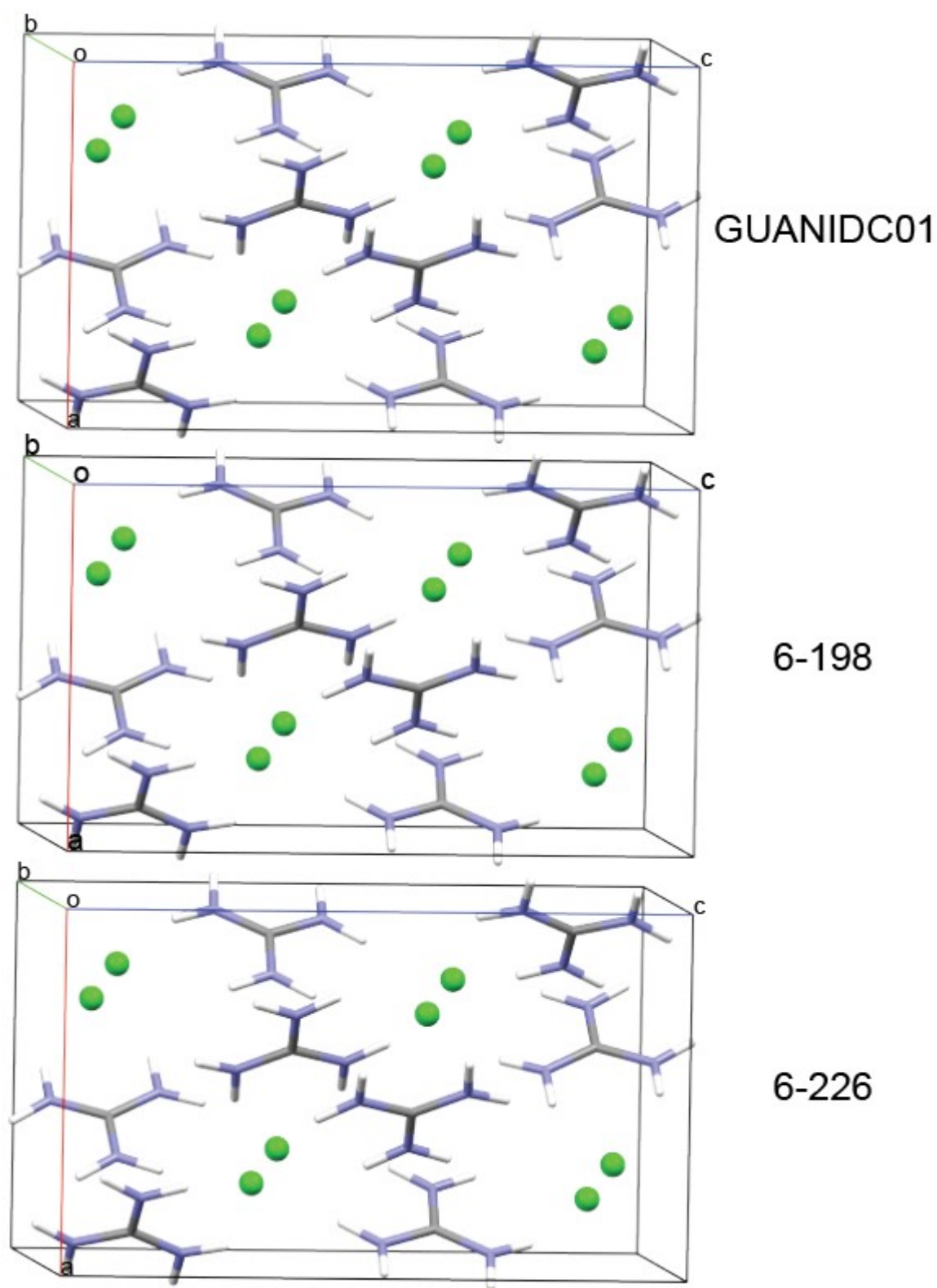


Figure S9. A comparison of the DFT-D2* geometry-optimized structural model of guanidine HCl derived from its known crystal structure (GUANIDC01) with two (from a set of 19) validated structural models, 6-198 and 6-226.

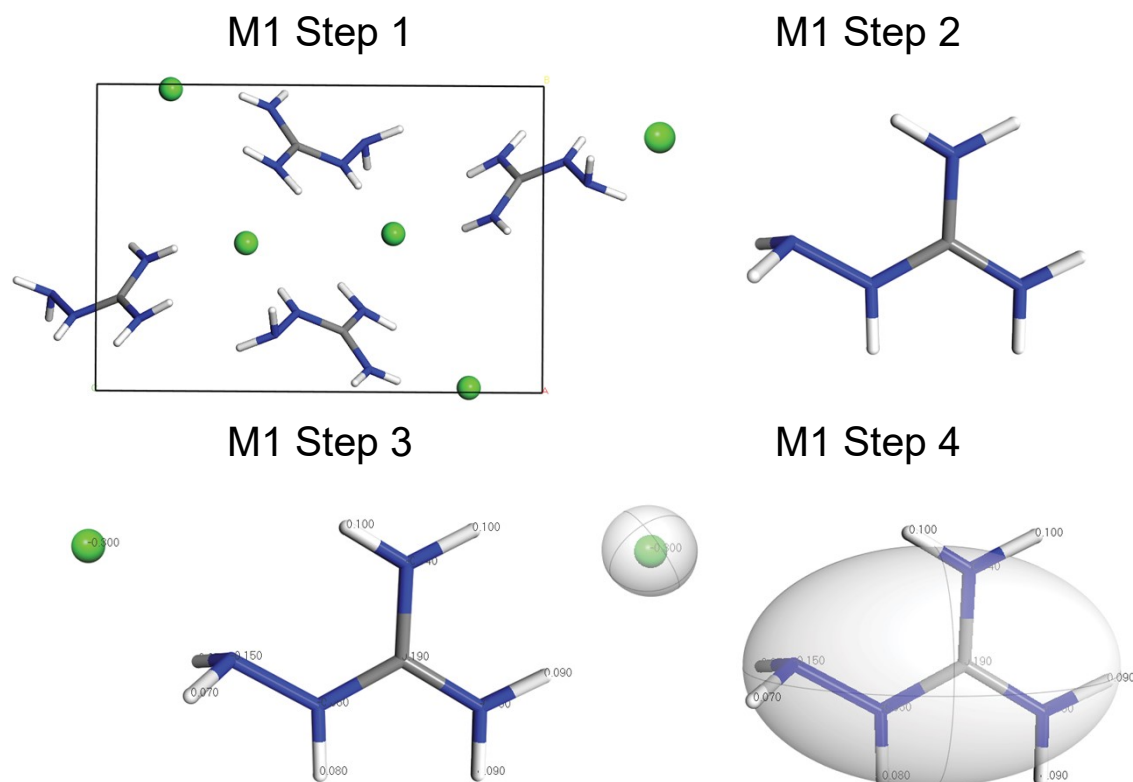


Figure S10. A walkthrough of the QNMXR-CSP protocol, Module 1, Stage 1 (Molecular Fragments and Motion Groups) for aminoguanidine HCl. M1 Step 1: obtain a known crystal structure (AMGUAC02). M1 Step 2: perform a DFT-D2* geometry optimization and unbuild the crystal structure. M1 Step 3: assign the Hirshfeld charges to the atoms. M1 Step 4: assign the motion groups.

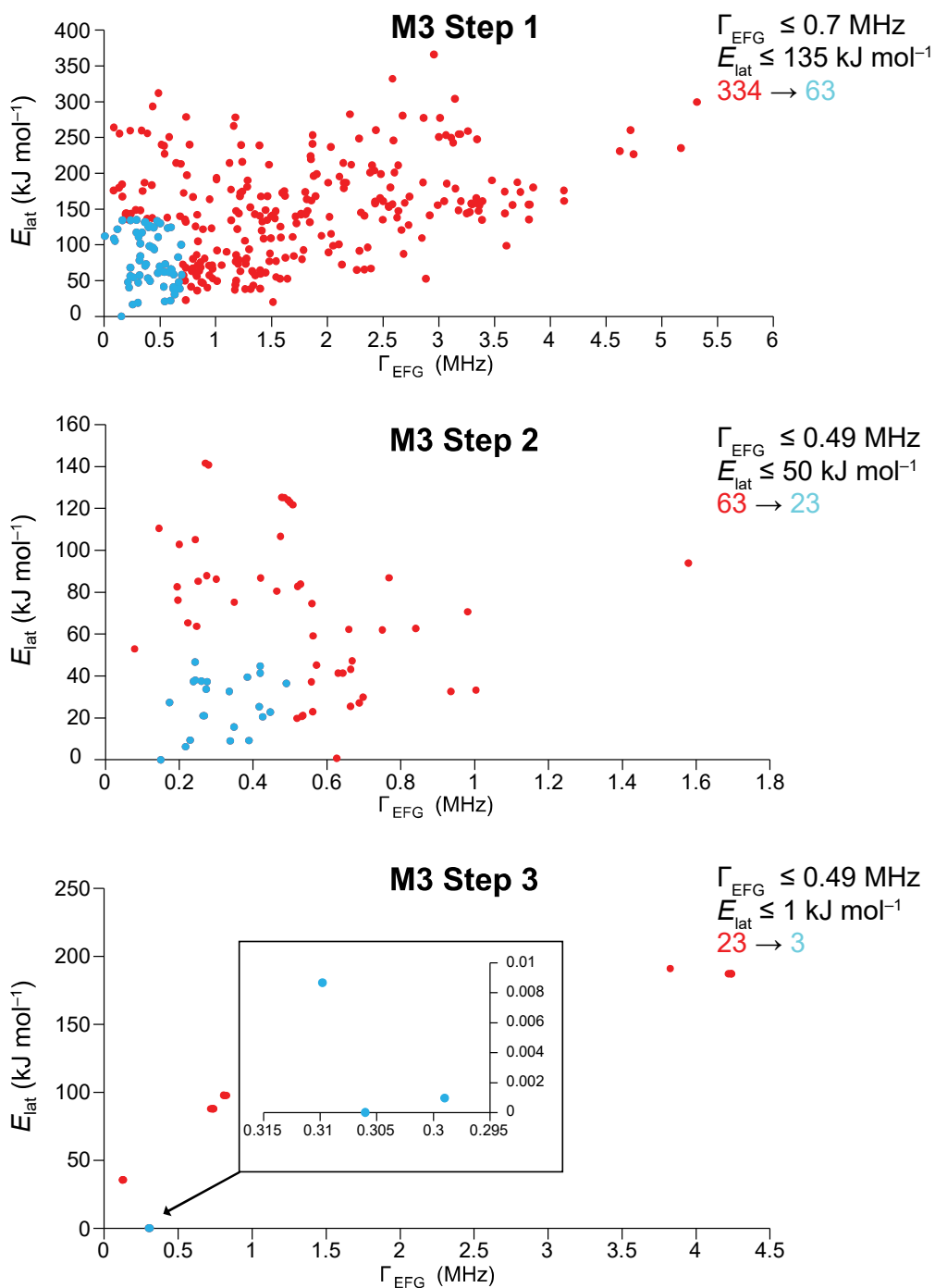


Figure S11. Scatter plots of E_{lat} vs. Γ_{EFG} for the walkthrough of the QNMRX-CSP protocol in Module 3, Stage 1, Steps 1-3 (QNMRX) for aminoguanidine HCl: Red and blue points denote discarded and retained candidate structures, respectively. The numbers of structures before (red) and after (blue) the application of benchmarked metrics are shown to the right. Shown in the inset of the scatter plot in M3 Step 3 are the structures that have $E_{\text{lat}} \leq 1 \text{ kJ mol}^{-1}$.

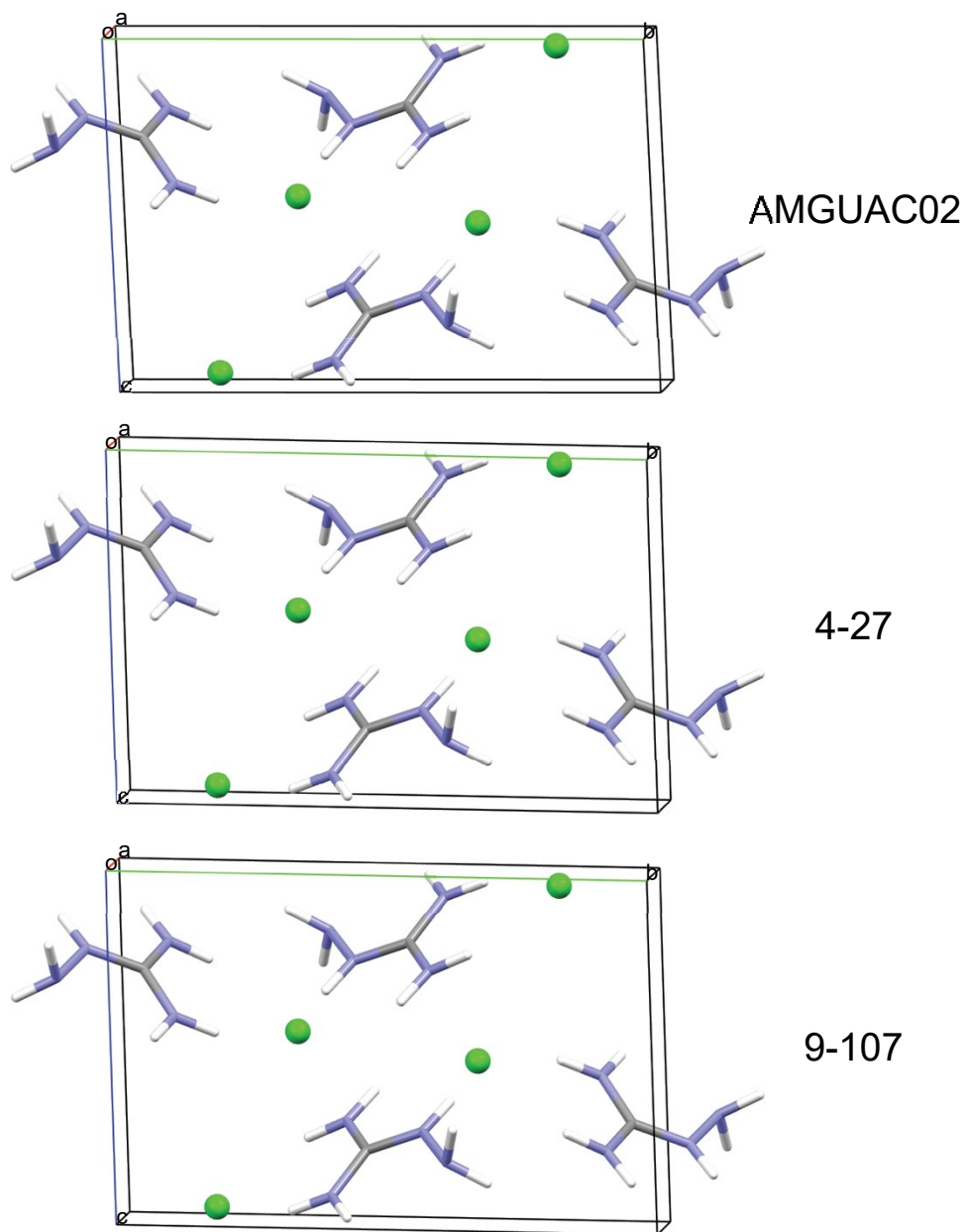
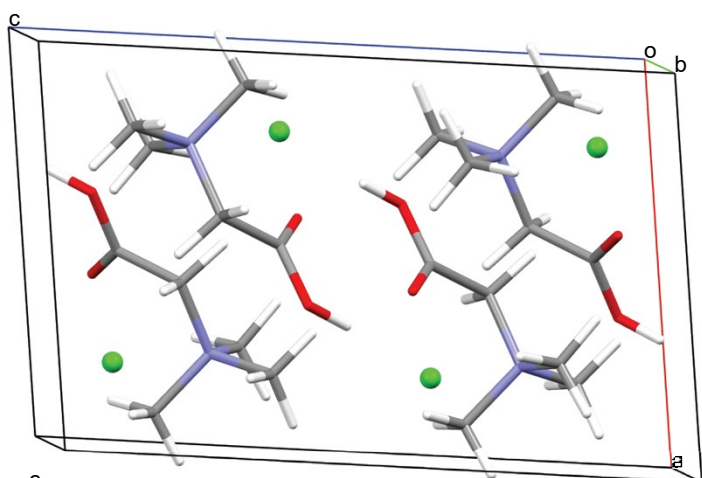
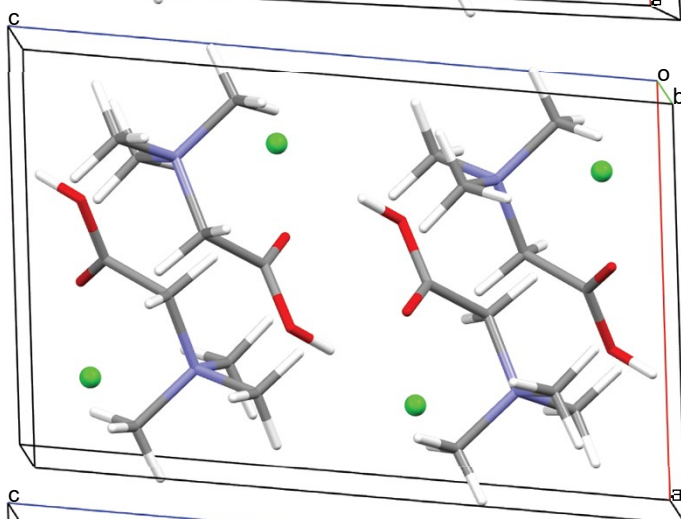


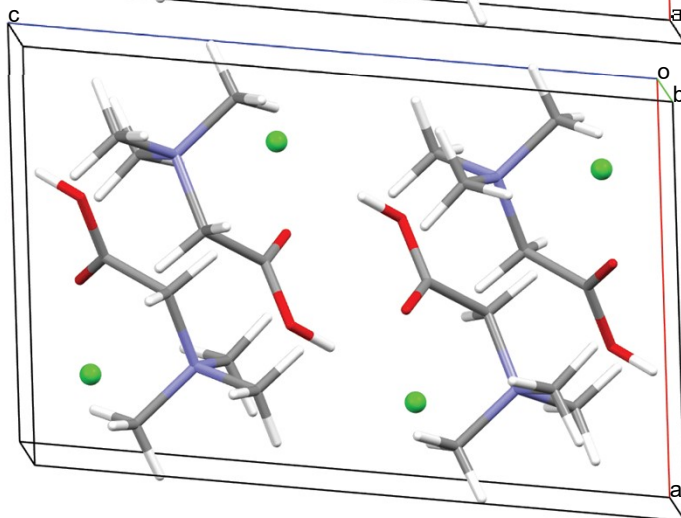
Figure S12. A comparison of the DFT-D2* geometry-optimized structural model of aminoguanidine HCl derived from its known crystal structure (AMGUAC02) with two (from a set of 3) validated structural models, 4-27 and 9-107.



BETANC01



P2
8-114



P3
10-269

Figure S13. A comparison of the DFT-D2* geometry-optimized structural model of betaine HCl derived from its known crystal structure (BETANC01) with one validated structural model each from S2 and S3, 8-114 and 10-269, respectively.

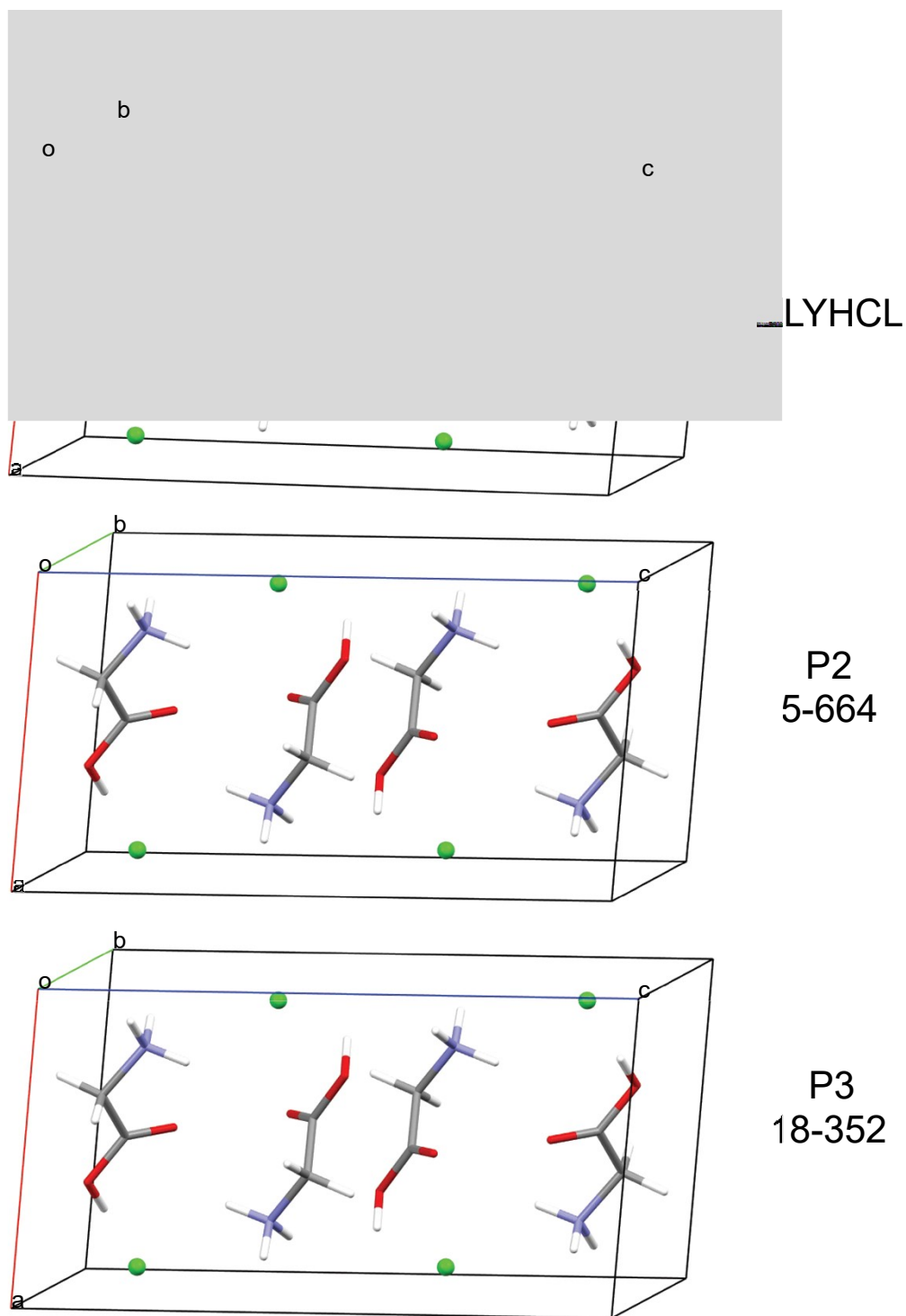


Figure S14. A comparison of the DFT-D2* geometry-optimized structural model of glycine HCl derived from its known crystal structure (GLYHCL) with one validated structural model each from S2 and S3, 5-664 and 18-352, respectively.

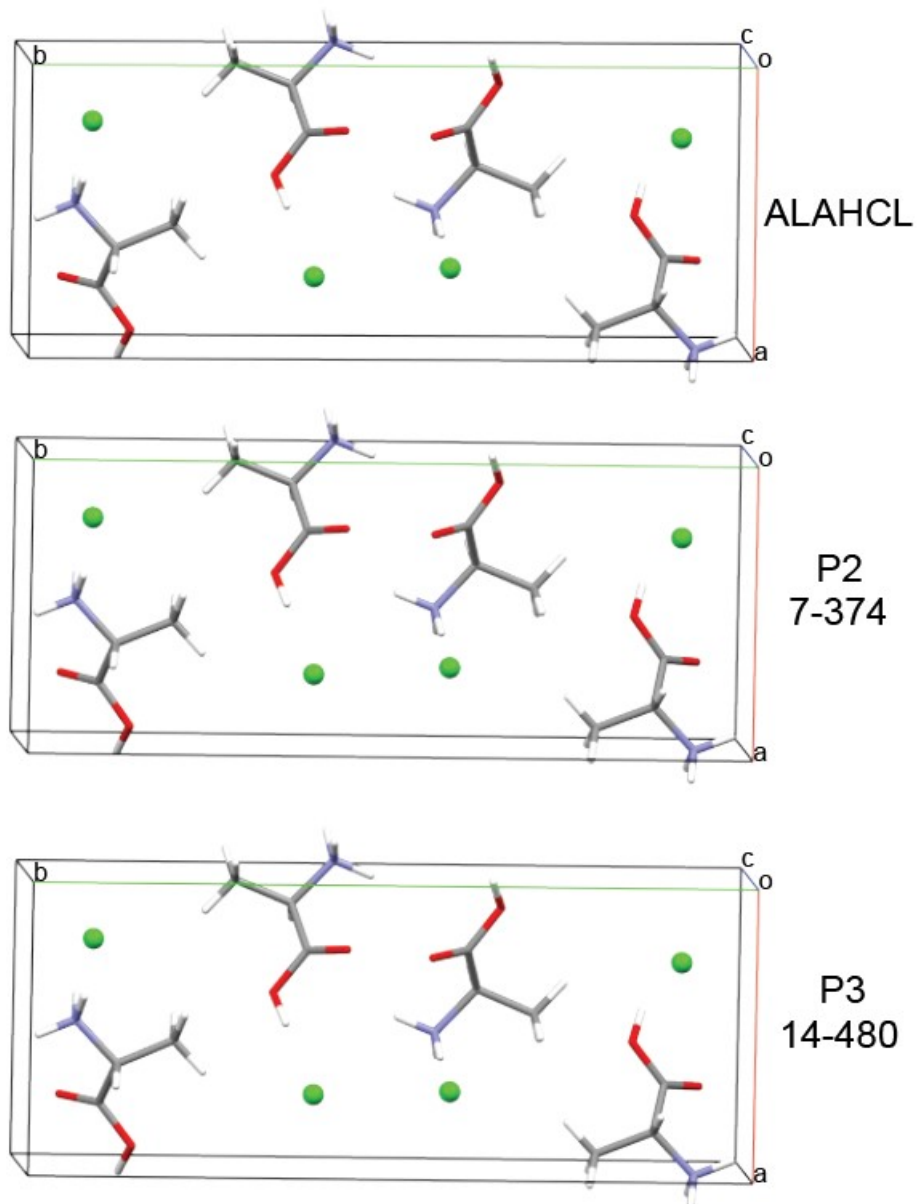


Figure S15. A comparison of the DFT-D2* geometry-optimized structural model of *D*-alanine HCl derived from its known crystal structure (ALAHCL) with one validated structural model each from S2 and S3, 7-374 and 14-480, respectively.

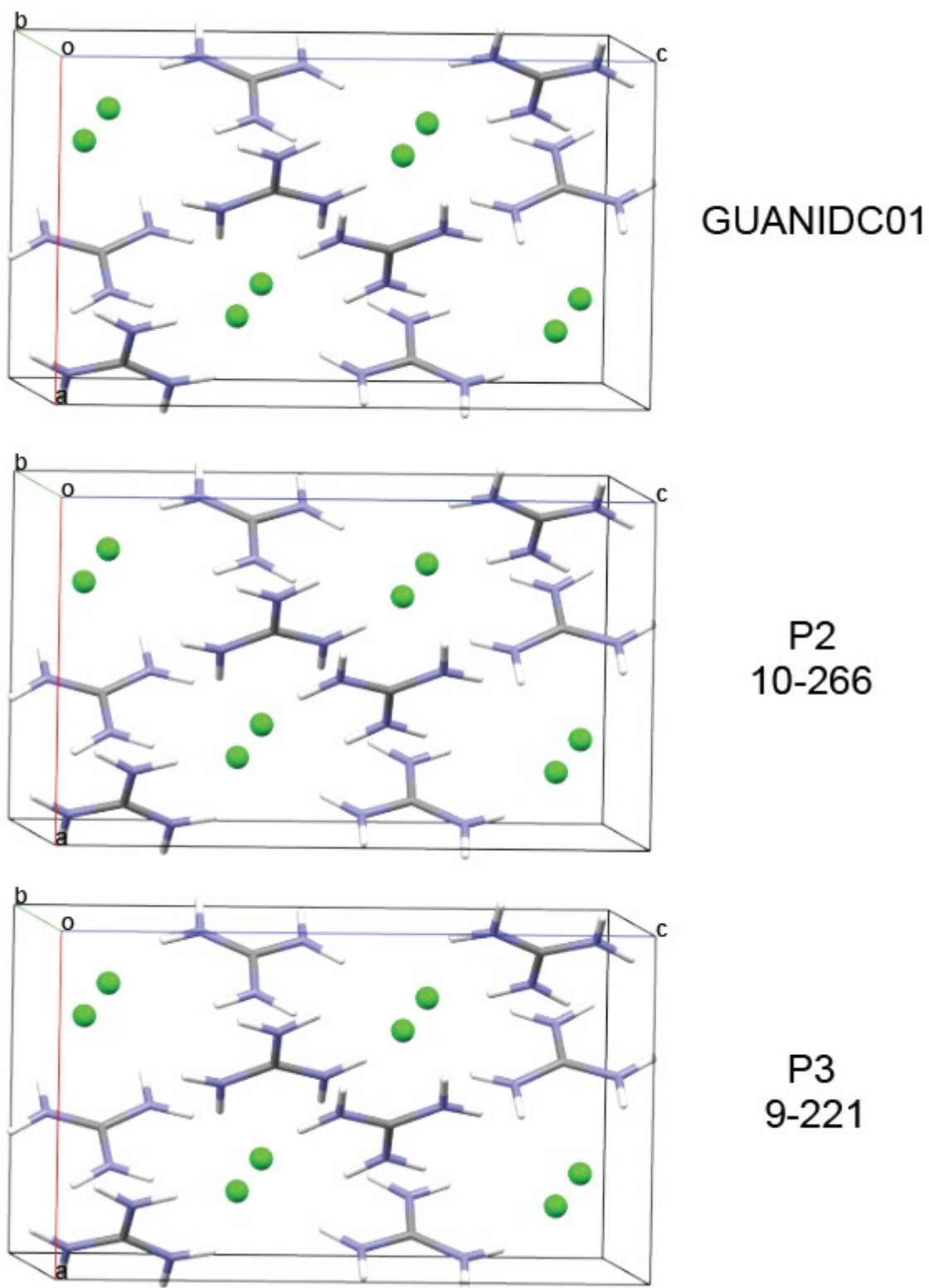


Figure S16. A comparison of the DFT-D2* geometry-optimized structural model of guanidine HCl derived from its known crystal structure (GUANIDC01) with one validated structural model each from S2 and S3, 10-266 and 9-221, respectively.

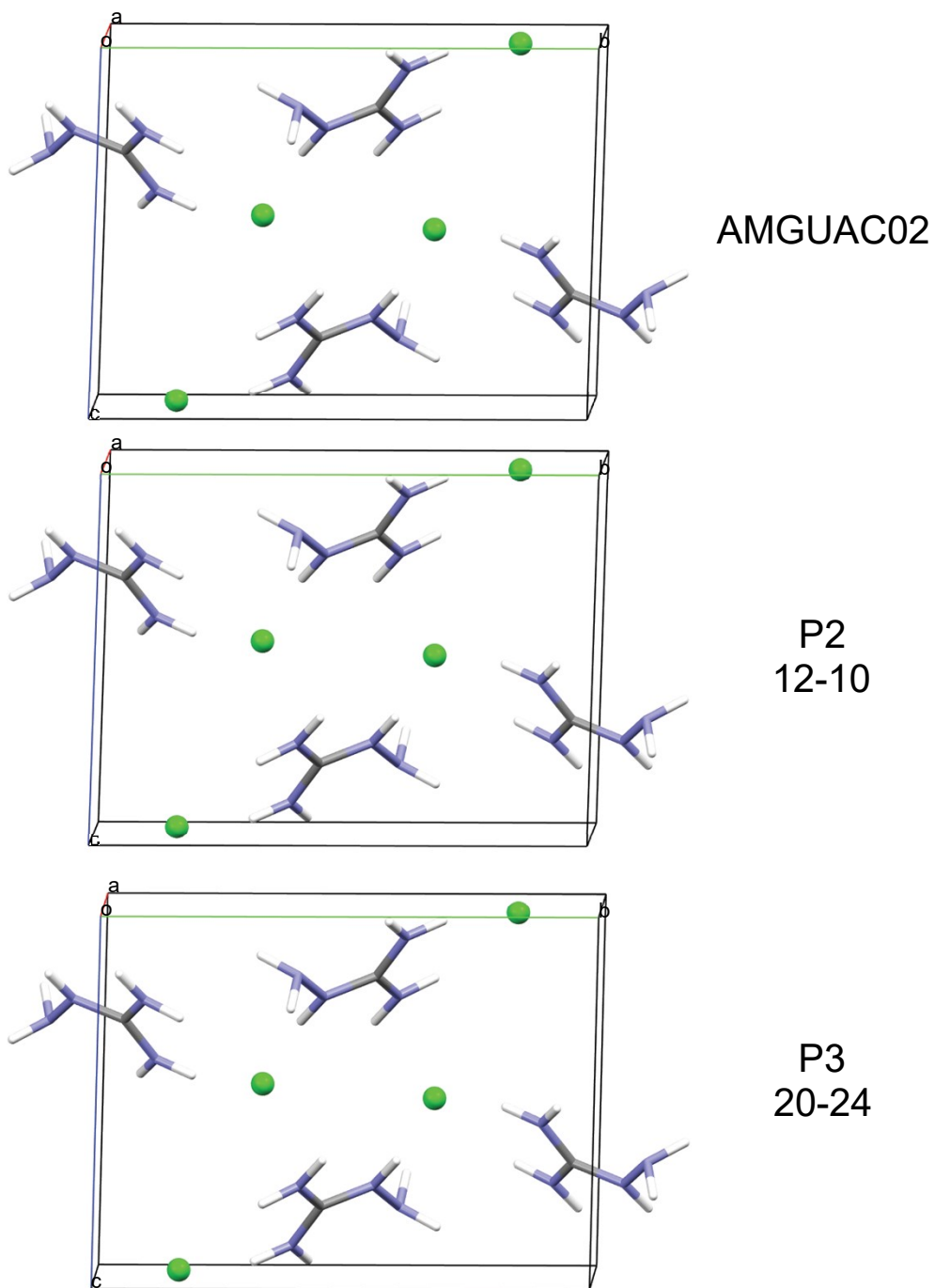


Figure S17. A comparison of the DFT-D2* geometry-optimized structural model of aminoguanidine HCl derived from its known crystal structure (AMGUC02) with one validated structural model each from S2 and S3, 12-10 and 20-24, respectively.

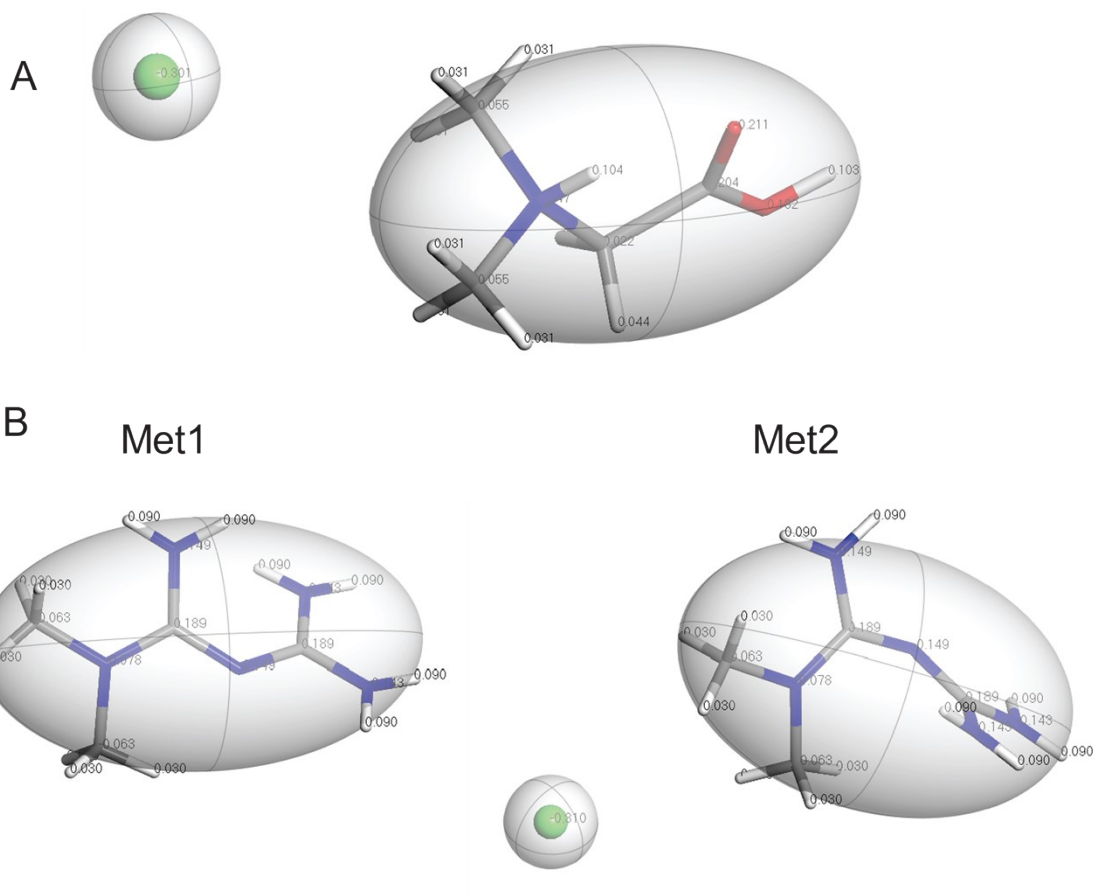


Figure S18. Molecular fragments of *N,N'*-dimethylglycine HCl (A, Dmg1 fragment is shown) and two conformers of metformin HCl (B, Met1 and Met2), with Hirshfeld charges and motion groups assigned.